SD 76-SA-0095-2

LANDSAT / MMS PROPULSION MODULE DESIGN TASK 4.4 - CONCEPT DESIGN FINAL REPORT

24 Sept 1976

Contract NAS5-23524

Prepared for

GODDARD SPACE FLIGHT CENTER
GREENBELT, MARYLAND 20771

ACCESSION NUMBER		DOCUMENT SECURITY CLASSIFICATION	
		UNCL.	

TITLE OF DOCUMENT

LANDSAT/MMS PROPULSION MODULE DESIGN
FINAL REPORT

LIMITATION USE ONLY

AUTHOR(S)

J. M. MANSFIELD, F. G. ETHERIDGE, J. INDRIKIS

CODE	ORIGINATING AGENCY AND OTHER SOURCES	DOCUMENT NUMBER
		SD 76-SA-0095

PUBLICATION DATE	CONTRACT NUMBER
24 SEPT 1976	NAS5-23524

DESCRIPTIVE TERMS

MODULAR SPACECRAFT, HYDRAZINE PROPULSION SYSTEMS, SHUTTLE PAYLOADS, EARTH ORBITING SPACECRAFT.

ABSTRACT

EVALUATIONS ARE PRESENTED OF ALTERNATIVE LANDSAT FOLLOW-ON LAUNCH CONFIGURATIONS TO DERIVE THE PROPULSION REQUIREMENTS FOR THE MULTIMISSION MODULAR SPACECRAFT (MMS). TWO BASIC TYPES WERE ANALYZED INCLUDING USE OF CONVENTIONAL LAUNCH VEHICLES AND SHUTTLE-SUPPORTED MISSIONS. IT WAS CONCLUDED THAT TWO SIZES OF MODULAR HYDRAZINE PROPULSION MODULES WOULD PROVIDE THE MOST COST-EFFECTIVE COMBINATION FOR FUTURE MISSIONS OF THIS SPACECRAFT. CONCEPTUAL DESIGNS OF THE SELECTED PROPULSION MODULES WERE PERFORMED TO THE DEPTH PERMITTING DETERMINATION OF MASS PROPERTIES AND ESTIMATED COSTS.

FOREWORD

This report is provided in accordance with the requirements of Contract NAS5-23524. The data and analyses were prepared by the Space Division of Rockwell International for the Goddard Space Flight Center of the National Aeronautics and Space Administration. The report is printed in three volumes:

I. Task 4.3 - Trade Studies

II. Task 4.4 - Concept Design

III. Appendix - Cost Analyses

The following individuals contributed to this report: R. Yee, F. Etheridge, B. Mahr, B. Brandt, M. Sandersfield, and J. Mansfield.

CONTENTS

ILLUSTRATIONS

DRAWINGS

TABLES

1.0 INTRODUCTION

The Multimission Modular Spacecraft (MMS) is being developed by the Goddard Space Flight Center to achieve cost savings in future unmanned earth orbiting space projects through the utilization of a Shuttle-compatible standardized modular spacecraft. One of the early missions being considered which might utilize this approach is a follow-on to the current Landsat. If adopted, this mission would potentially be the first MMS application to require a propulsion subsystem. The Space Division of Rockwell International has performed a series of analysis and design tasks to define a modular propulsion subsystem concept which will be compatible with the MMS and will satisfy the Landsat follow-on mission propulsion requirements.

The initial portion of this effort concentrated on evaluation of alternative Landsat follow-on launch configurations to establish propulsion requirements and performance of trade studies of the propulsion subsystem elements to select the most cost effective sizing approach to meet variations in requirements. Volume I of this report summarizes the analyses which were utilized in preparation of conceptual designs of the propulsion module. These conceptual designs and associated analyses are summarized in this volume.

2.0 SUMMARY AND CONCLUSIONS

As described in Volume I of this report, two basic types of Landsat follow-on missions have been analyzed to derive the propulsion requirements. These include utilization of a conventional launch vehicle such as the Delta 3910 for launch and delivery to the operational orbit or, alternatively, use of the Space Shuttle to deliver and/or retrieve the spacecraft at some intermediate altitude, with dependence or the MMS propulsion to provide transfer to the operational orbit. The use of the intermediate altitude in the Shuttle-supported mode is cost effective based on the current approach to computing the relative portion of Shuttle launch costs to be borne by an individual payload.

These two missions have led to two distinctly different propulsion modules for the MMS. Conceptual designs for these have been prepared in sufficient depth to establish structural configuration, cost, and mass properties. Optional arrangements have been identified for increasing the propellant capacity of the Delta-launched version, including concepts which project into the central volume of the MMS. A concept for control and monitoring of the module has been derived and a preliminary examination of the plume envelope has been conducted.

The most significant drivers on the configurations other than the propellant requirements were found to be the length available inside the adaptor to the Delta launch vehicle, the provisions for on-orbit exchange, the electrical integration requirements, and capabilities and shape factors of existing hardware. All established mission requirements can be met by the conceptual designs, but further design iterations appear desirable as the mission requirements and servicing system evolve.

3.0 DELTA MISSION CONFIGURATIONS

3.1 REQUIREMENTS

The mission analyses described in Volume I of this report defined the propellant requirements for the Delta-launched Landsat follow-on mission in accordance with the parameters defined in the work statement. The total requirement of 61.1 pounds of hydrazine included allowances for correction of initial orbit injection errors, maintaining the ground track within 5-Km for three years, performing four stabilization maneuvers, and operating in a safe hold mode for 30 days awaiting emergency retrieval. This was the baseline requirement for the design effort on the propulsion module for this mission, designated Spacecraft Propulsion Subsystem I (SPS-I). It was recognized, however, that subsequent analyses might show a need for additional orbital adjustments so a guideline was established to examine options for maximizing the propellant capacity within the volumetric constraints.

The volumetric constraints arose from two primary sources, the module exchange process and the launch vehicle adapter. The module exchange mechanism has not been completely defined at this time, but it has been established that the modules will be withdrawn radially to the spacecraft centerline. The module retention mechanism concept has been selected, and preliminary sizing of the module interfacing device which actuates the latches has been performed. These constraints, together with the overall geometry and capabilities of the MMS structure, led to a propulsion module configuration attached at three brackets to the aft structure of the spacecraft, and limited dimensionally to permit withdrawal. It should be noted that if no servicing on orbit is required, some of the dimensional constraints are removed. Options capitalizing on this feature are described later.

The launch vehicle adapter encloses the propulsion module and therefore constrains the overall geometry. The parameters defined during the study for the dynamic envelope were an overall length of 18.5 inches, an upper diameter of 55.0 inches, and a lower diameter of 52.0 inches to allow for tip-off excursions. Subsequent design development by the launch vehicle contractor

established that this envelope could be penetrated selectively in certain radial directions. This may become desirable as the propulsion module and module exchange mechanism designs mature, particularly for the latch operators.

3.2 SPS-I DESIGN CONFIGURATIONS

These constraints, together with other guidelines such as use of the "standard" MMS electrical connector, were combined to produce the initial layout shown in Drawing 42623-1. This drawing depicts the arrangement as it would generally appear looking forward and from the side. It was developed primarily to illustrate the interfaces of the propulsion module with the bottom of the spacecraft, the module exchange process, and the launch vehicle adapter envelope. The orientation of the rocket engine modules (REM's) is dictated by the location and orientation of the Attitude Control Subsystem (ACS) module. Note that this orientation results in one of the 0.2-lb thrusters pointing generally in the direction of the umbilicals and berthing probe at upper right. A further detail of this geometry is shown on the right side of the drawing and is analyzed further in Section 6.0.

Orientation of the supporting brackets, electrical connector, and tanks is driven by the Shuttle landing loads. The primary load direction is along the $-Z_M$ axis (toward the bottom of the drawing), and it is desirable to carry the loads symmetrically. The attachment system shown utilizes two bolts on the module which engage nuts on the spacecraft. These, together with shear lips on the interface plane allow reaction of both $\pm X_M$ and Z_M loads at these points. At the apex point, the electrical connector is guided into engagement by two pins which engage sockets on the spacecraft side and react $\pm X_M$ and $\pm Y_M$ loads. A basic two tank arrangement is shown with alternates of one or three tanks.

The tanks shown are of 16.5-inch internal diameter, positive expulsion tanks. They are a version of the TIP-2 tank modified to incorporate an equatorial pressurization port. The necessity for this modification can be seen in the side view where the close tolerances top and bottom are shown. The principal structural member shown is a four-inch bulkhead of honeycomb which supports the tanks, the support brackets, and the thrusters. Not shown are the electronics required for system control and monitoring.

The envelope constraints on the module interfacing device (MID) of the module exchange mechanism (MEM) also are shown on the drawing. The requirement to reach in under the Electrical Power Subsystem (EPS) module to engage the latches on the propulsion module is a unique driver on the MEM. As mentioned above, it may be desirable to extend the latch driver interface outboard to relieve this requirement on the MEM.

The requirement for clearance between the MID and the EPS module requires that the latch centerlines be positioned well below the interface plane between the propulsion module and the MMS module support structure. This provides a ready path for the cabling from the umbilicals to be routed along the bottom edge of the support structure, around one or both sides of the latch bracket, and into the central cavity. The most difficult portion of the cabling appears to be the initial routing prior to approaching the propulsion module. There, careful attention is required to provide withdrawal clearance for the adjacent modules, avoid interference with the Delta adaptor fitting, and stay clear of any provisions (bumpers) required on the corners of the adjacent modules for dynamic damping.

After a review of the initial layout and system analysis with the GSFC, it was decided that the following guidelines would be adopted for the conceptual design of the SPS-I:

1. Layout drawings will be based on the use of the LCSO 0.2-lb and Hamilton Standard 5.0-lb thrust engine configurations as examples of typical geometries.

2. No latch valves or pressure transducers will be used at individual tank outlets.

3. Layout drawings will show three modified TIP-2 tanks; the pressurization lines to each tank will be manifolded as will the fuel lines.

The key features of the proposed baseline module are simplicity and low cost. Design simplicity is achieved by using minimal number of proven components with little or no redundancy. Low cost is implicit in this approach.

The schematic of the SPS-I following these guidelines is shown in

Figure 1 and the design concept on Drawing 42623-3 and Figure 2. The propulsion elements include the following:

- Three Pressure Systems, Inc. (PSI), Modified TIP-2 tanks
- Two LCSO fill and drain valves
- Three temperature transducers
- One LCSO pressure transducers
- One Wintek System filter
- Six LCSO latch valves
- Twelve LCSO 0.2-pound thrusters
- Four Hamilton standard 5.0-pound thrusters

The tankage for the SPS-I is a slightly modified TIP-2 design. The modifications are external and in no way impact the internal arrangement or diaphragm. In the modified TIP-2 tank, the first change involves moving the gas port from the polar region to the equator. PSI suggested the change as a means of reducing tank length and indicated the equatorial gas port has been used on hydrospace diaphragm tankage. The second modification, was required by the need to increase the burst to operating ratio to 4.0. This change would greatly facilitate the tankage fueling and pressurization operations at ETR, thereby reducing overall program costs. Implementing the 4:1 criteria would require an increase in tank wall thickness to provide a burst pressure of 1600 psia. The MVM tankage, one of the PSI 16.5-inch tankage family, was qualified at a burst pressure of 1580 psia. PSI has indicated that no difficulty would be anticipated in modifying and qualifying the TIP-2 tank to this criteria. The only penalty would be a minor increase in weight (12.2 pounds as compared with 11.5 pounds of the existing TIP-2 tank) and in non-recurring cost. The non-recurring cost increase is estimated to be equal to 25 percent of the recurring cost of one tank. All SPS-I tanks are manifolded and filled through a single gas fill and drain valve and a single propellant fill and drain valve.

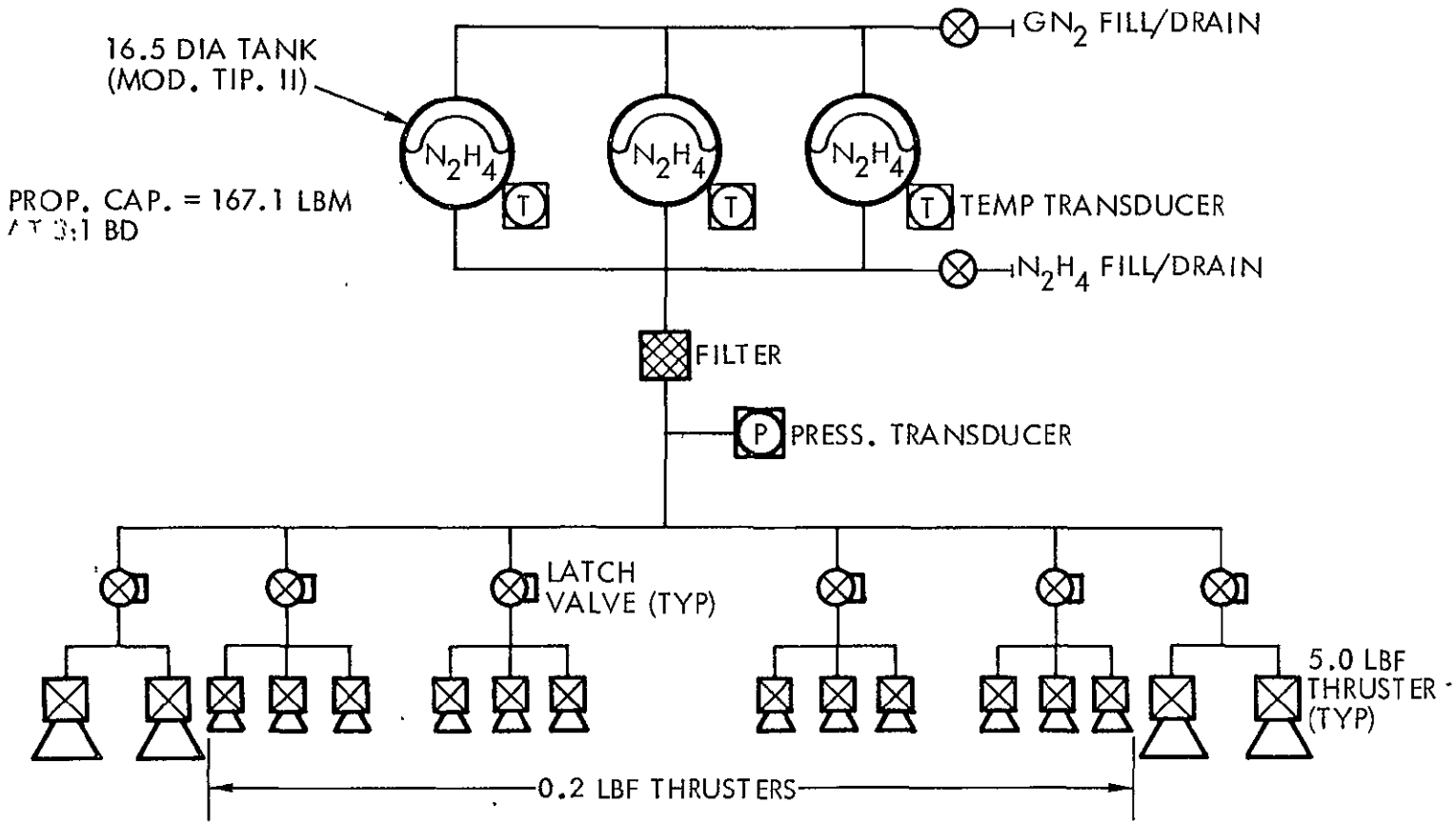

Figure 1. SPS-I Schematic

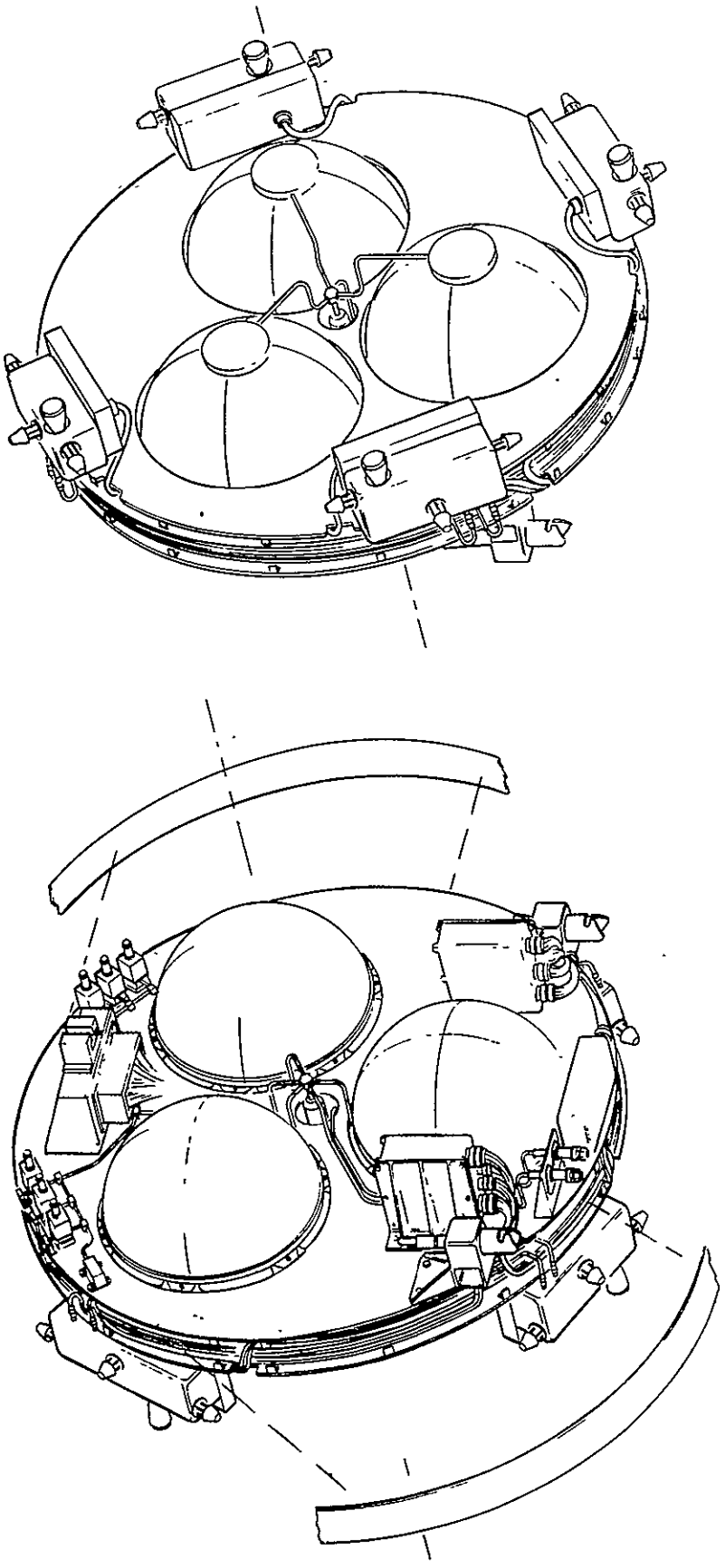

Figure 2. SPS-1 Perspective

Latch valves are used for thruster isolation in the event a propellant control valve fails open. Candidate latch valves include the LCSO design by Marquardt as discussed in Volume I, Section 7, and the Hydraulic Research torque motor operated magnetic latching valve used on the CTS and currently on the GPS. The Hydraulic Research design provides a flow rate considerably higher (0.06 pps), than that required by the SPS-I where as the Marquardt design is marginal (0.038 pps) even if it can be qualified to the required flow rate (0.043 pps). Use of the LCSO valve at the 0.038 pps flow rate would result in a beginning-of-mission thrust loss at approximately 12 percent. The latch valve configuration shown on Drawing 42625-3 is the LCSO Marquardt configuration. The Hydraulic Research design is a highly desirable alternate and, as discussed in the cost analysis appendix, is available at a lower cost than the LCSO component. The tank temperature transducer is a standard off-the-shelf item and one per tank is desirable to insure that the hydrazine temperature can be monitored. The GPS temperature transducer, manufactured by RJF Corporation, Hudson, N. H., SD P/N MC449-0195, would be an acceptable item for this purpose. The thrusters shown in Drawing 42623-3 are the Rocket Research LCSO thruster and the Hamilton Standard 5.0 thrust IUE engine. Details on the LCSO thruster are presented in Volume I Section 7; additional details on the Hamilton Standard engine are presented below.

The Hamilton Standard 5.0 lbf thruster is one of the REA 16 series of thrusters which have been qualified and flown on 16 spacecraft. The propellant valve for the 5.0 lbf thruster is a single seat, solenoid operated valve furnished by Wright Components. The basic thruster consists of a trim orifice, injector tubes, diffusers, thermal standoff, reaction chamber, and exhaust nozzle. The transition tube is welded to the inlet of the thruster and provides a flange for attachment of the propellant valve.

Six capillary tubes are used, as in all other REA 16 thrusters. At the end of each capillary tube, projecting into the catalyst bed, is a dual screen diffuser. The diffuser is used to uniformly distribute the propellant to the catalyst bed and the screen is employed to prevent catalyst fines from migrating upstream especially during thruster vibration.

Four identical rocket engine modules (REM) are provided to effect pitch, yaw, and roll control using the 0.2 lbf thrusters and delta velocity maneuver using the 5.0 lbf thrusters. Each REM contains three 0.2 lbf thrusters and one 5.0 lbf thruster. The three 0.2 lbf thrusters are connected to one latch valve and two 5.0 lbf thrusters from opposing REMS are connected to another latch valve. Firing of the individual thruster is controlled by the actuation of a normally closed solenoid valve. In the event of a failed open thruster, the latch valve is actuated closed to terminate the propellant flow to the failed thruster as well as those thrusters that are controlled by the same latch valve.

Figure 3 illustrates the arrangements of the thrusters in the REM. A right-angle nozzle configuration was adopted for the 5.0-pound thruster in order to stay within the geometrical limits. As shown, the electronics to control and monitor the REM thrusters and thermal control are packaged immediately adjacent to the REM in order to minimize the wire length and EMI (see Section 5.0). Dynatube mechanical joints are shown at the REM interface to permit ready replacement of the entire REM.

Space Division (SD) has a broad range of experience with Dynatube fittings. This component was used on the Apollo program and is currently employed on several Shuttle subsystems, including the hydrazine auxiliary power unit. If properly prepared, installed, and checked, it has been found that the Dynatube fitting is extremely reliable and does not require redundancy. When handled correctly, the reliability of a Dynatube connection is comparable with that of a brazed or welded joint. SD experience has indicated that when problems with the Dynatube fitting have occurred, it has generally been due to improper alignment and/or lack of support of the propellant lines adjancent to the connector. SD believes that an entirely satisfactory utilization of Dynatube fitting on the MMS hydrazine propulsion system can be achieved if the following criteria are implemented:

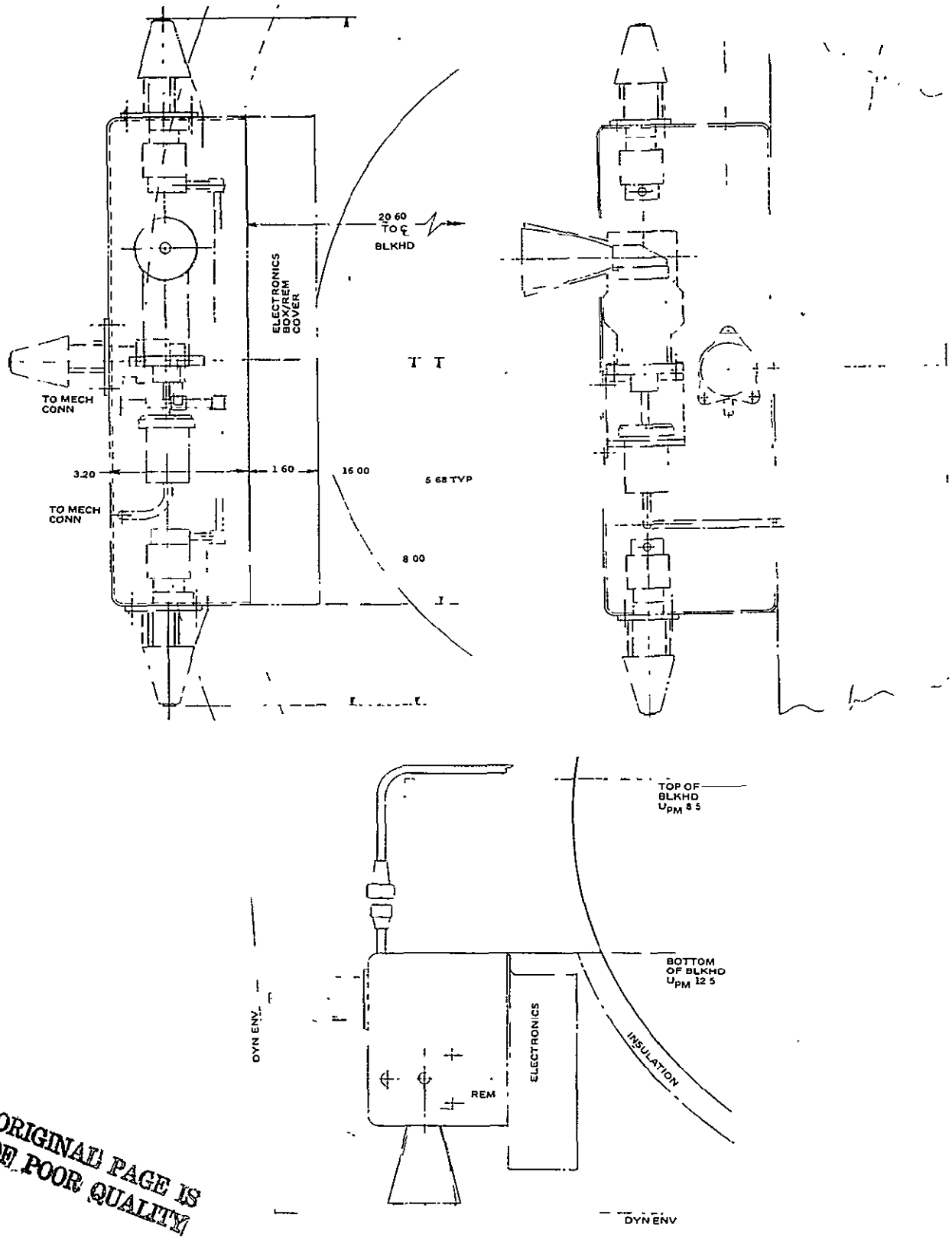

Figure 3. Rocket Engine Module (REM)

- Test
  - Establish torque values to meet leakage requirements
  - Determine allowable vibration levels as a function of line size
  - Determine leakage vs. temperature characteristics
- Design
  - Fitting ends are welded to cres tubing
  - Adequate support of lines and mating parts to prevent flexure during vibration
  - Proper torque values specified
  - Mating sealing surfaces polished to an 8 RMS finish
  - Joints safety wired for reliability
  - Line size limited to 1/2 inch diameter maximum for N_2H_4 service
- Process Control
  - Fixtures used to protect sealing surfaces during assembly
  - Adequate inspection data specified for checking centerline to centerline alignment of tube with mating part during assembly
  - All joints checked to a requirement of 1×10^{-4} SCCS, actual, helium, at system operating pressure

In the event GSFC elects not to use the Dynatube fitting, the SD suggests that a NAVAN type flange seal be investigated as a means of providing redundant sealing.

Drawing 42623-3 also illustrates the location and arrangement of the other system elements including the electrical connector, the latching valves, pressure transducer, system filter, fill and drain valves, remote interface units (RIU), and electronics to control and monitor the non-REM elements. All elements except the REM's are mounted on the forward face of the bulkhead to minimize their environmental exposure including plume impingement. All plumbing and wiring to the REM's is routed through the channel which is the closeout member for the bulkhead and is covered by a thermal protective cover. The relationship between the latching valves and the thrusters is shown in Table 1.

Table 1. Thruster/REM Relationship to Latch Valves
(Ref. Drawing 42623-3, Zone 18)

Latch Valve	Thruster/REM Controlled
1	REM D
2	5.0-lb Thrusters D-1 and B-1
3	REM A
4	REM B
5	5.0-lb Thrusters A-1 and C-1
6	REM C

The concept for the attachment to the MMS structure was modified somewhat from the earlier layout. Drawing 42623-3 shows a concept which utilizes a "dovetail fitting" on the same bracket which holds the electrical connector in place of the two pins shown on Drawing 42623-1. The advantage of this modification is that it allows engagement of the dovetail with a guide rail on the MMS (or module magazine) early in the module insertion motion where visibility is better and ensures accurate tracking of the module electrical connector and structure supports to their mating parts. This is particularly important for the insertion into the module magazine where the apex point will be hidden from the operator.

Preliminary sizing of the propulsion module structure was accomplished using the NASTRAN computer program and a simple structural model. CRT projections of the model giving node point and element notations are shown in

Figures 4 and 5. The model contains 27 node points and 46 elements. Bar (CBAR) elements are used to represent the propellant tank attach rings, the bulkhead outer closeout ring, and the MSS attach fittings. Triangular (CTRIA1) and rectangular (CQUAD1) honeycomb plate elements are used to represent the bulkhead. Initial modeling was based on a 4-inch thick bulkhead and then revised to reduce the bulkhead thickness to 3 inches. The resulting element section properties are given in Figures 6 through 9. 7075-T73 aluminum was used for all bar elements, and 7075-TG aluminum was used for the plate elements.

Using the loading and reaction system shown in Figure 10 and MMS criteria, a static analysis of the model was run for Delta launch and orbiter loading conditions. Each load condition was run with the possible 1, 2, or 3 propellant tank combinations. Structural mass and propulsion system mass exclusive of the propellant and propellant tank mass was distributed uniformly on the bulkhead plate elements and given inertial loading by means of the NASTRAN gravity loading system. The propellant tank loads were distributed equally to each tanks' bulkhead attach points. The resulting maximum stresses reaction loads and deflections are summarized in Table 2. These data show that the concept with a 3-inch thick bulkhead is more than sufficient for the static load and deflection criteria. Also, the structure can be resized to reduce weight even when dynamic effects are included in the analysis.

Mass properties were estimated for the SPS-I configuration as shown in the following computer printout. These data assume the use of a 3-inch thick bulkhead and the above structural analysis. Table 3 presents a summary of the data for the version with two tanks and also shows the net change in weight and c.g. if the third tank is added. The two tanks are shown with a total propellant load of 64 pounds which approximates the requirement for the defined mission but is considerably below their capacity. This situation results because the maximum capacity of a single tank at a 3:1 blow-down ratio is 55.7 pounds. If a single tank were used to contain the minimum mission requirement of 61.1 pounds the corresponding blow-down ratio would be $\sim$ 3.6:1.

The center of gravity axis systems shown in the computer printout (Table 4) is based on the x axis Sta. 500 at the centerline of the spacecraft transition adapter. The y and z axis Sta. 0 have been taken as 500 inches from the spacecraft geometric centerline. In the mass properties summary of Table 3 the y and z c.g.'s are shown in reference to the geometric axis (i.e., the 500-inch bias is removed).

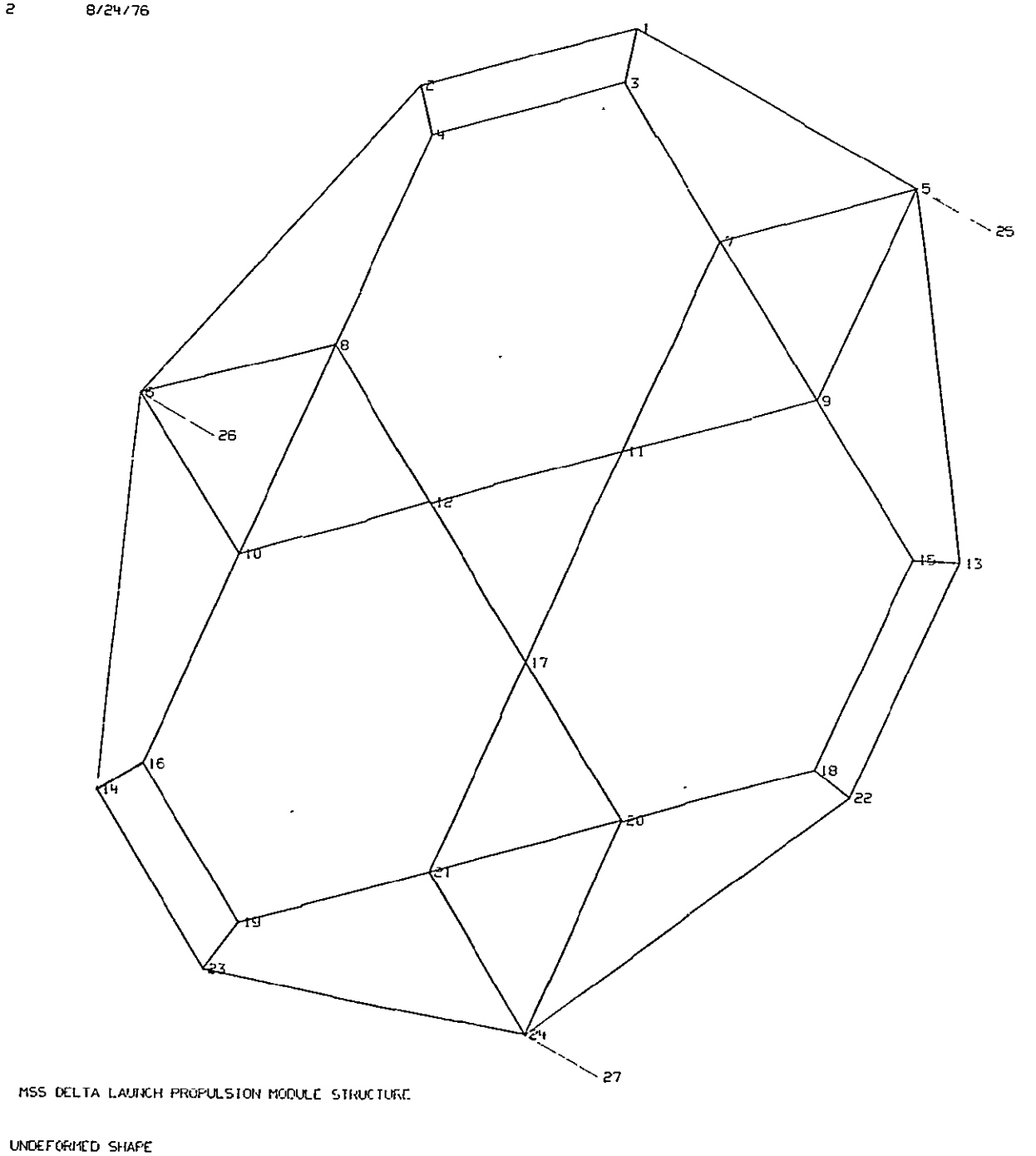

Figure 4. Structural Model Node Point Notation

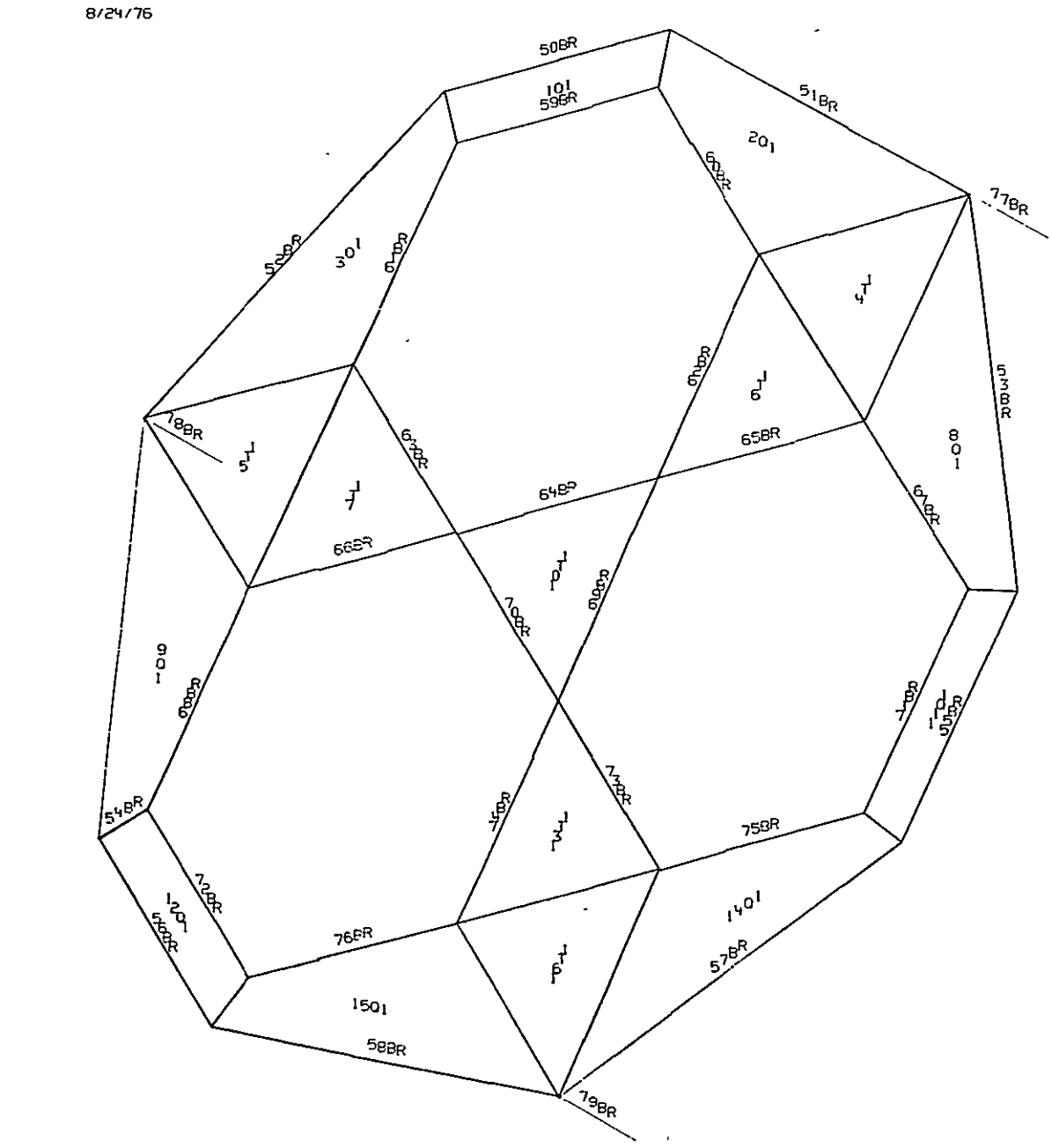

Figure 5. Structural Model Element Notation

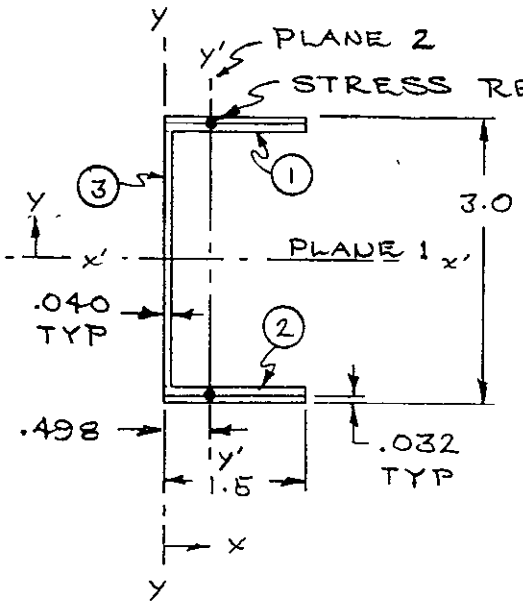

ELEMENT	b	t	y	x
1	1.5	.072	1.464	.75
2	1.5	.072	-1.464	.75
3	.04	2.856	0	.02

$I_1 = I_{y'y'} = 0.0803\ IN^4$

$I_2 = I_{x'x'} = 0.5407\ IN^4$

$A = 0.3302\ IN^2$

$J = 4.34 \times 10^{-4}\ IN^4$

Figure 6. Outer Ring Bar Elements

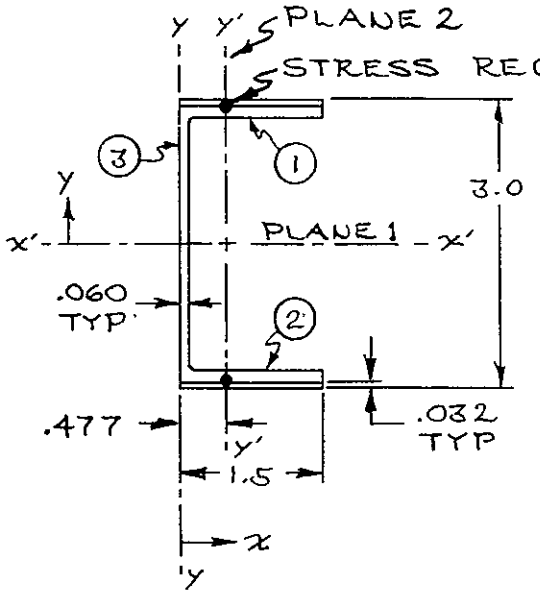

ELEMENT	b	t	y	x
1	1.5	.092	1.454	.75
2	1.5	.092	-1.454	.75
3	.06	2.816	0	.03

$I_1 = I_{y'y'} = 0.1061\ IN^4$

$I_2 = I_{x'x'} = 0.6953\ IN^4$

$A = 0.4450\ IN^2$

$J = 9.81 \times 10^{-4}\ IN^4$

Figure 7. Inner Rings Bar Elements

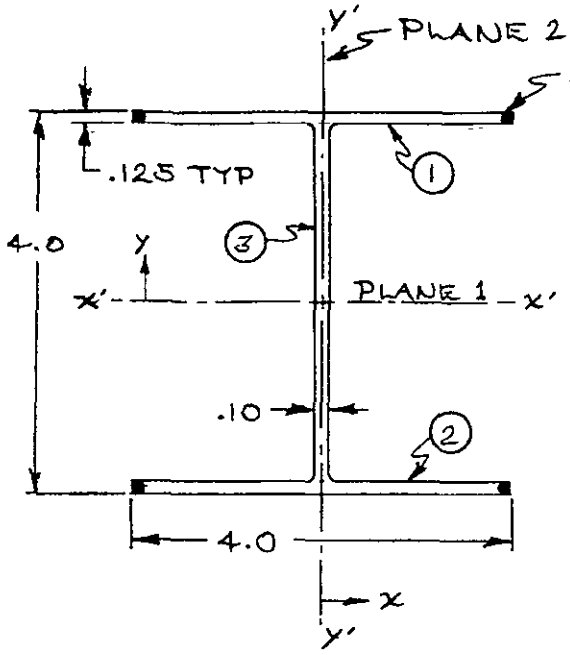

ELEMENT	b	t	y	x
1	4.0	.125	1.9375	0
2	4.0	.125	-1.9375	0
3	.10	3.75	0	0

$I_1 = I_{y'y'} = 1.3336\ IN^4$

$I_2 = I_{x'x'} = 4.1947\ IN^4$

$A = 1.3750\ IN^2$

$J = 6.46 \times 10^{-3}\ IN^4$

Figure 8. Bulkhead Attach Fittings Bar Elements

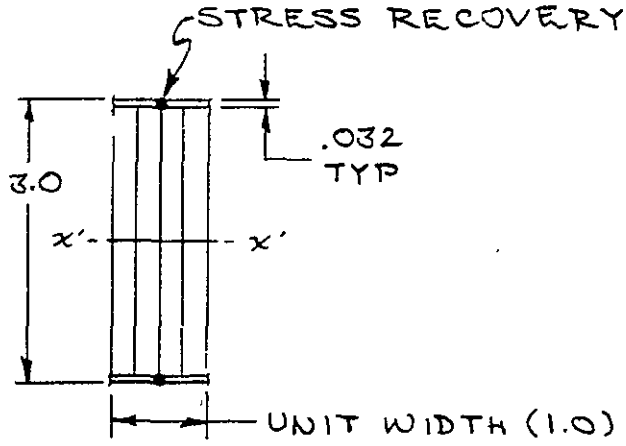

$I_{xx'} = 0.1409\ IN^4/IN$

$A = 0.0640\ IN^2/IN$

CORE:

- 5052-H39 Al.
- 3/16 CELL
- 0.0015 FOIL
- 4.4 LB/FT^3
- $h_c = 2.936$ IN

Figure 9. Honeycomb Bulkhead Plate Elements

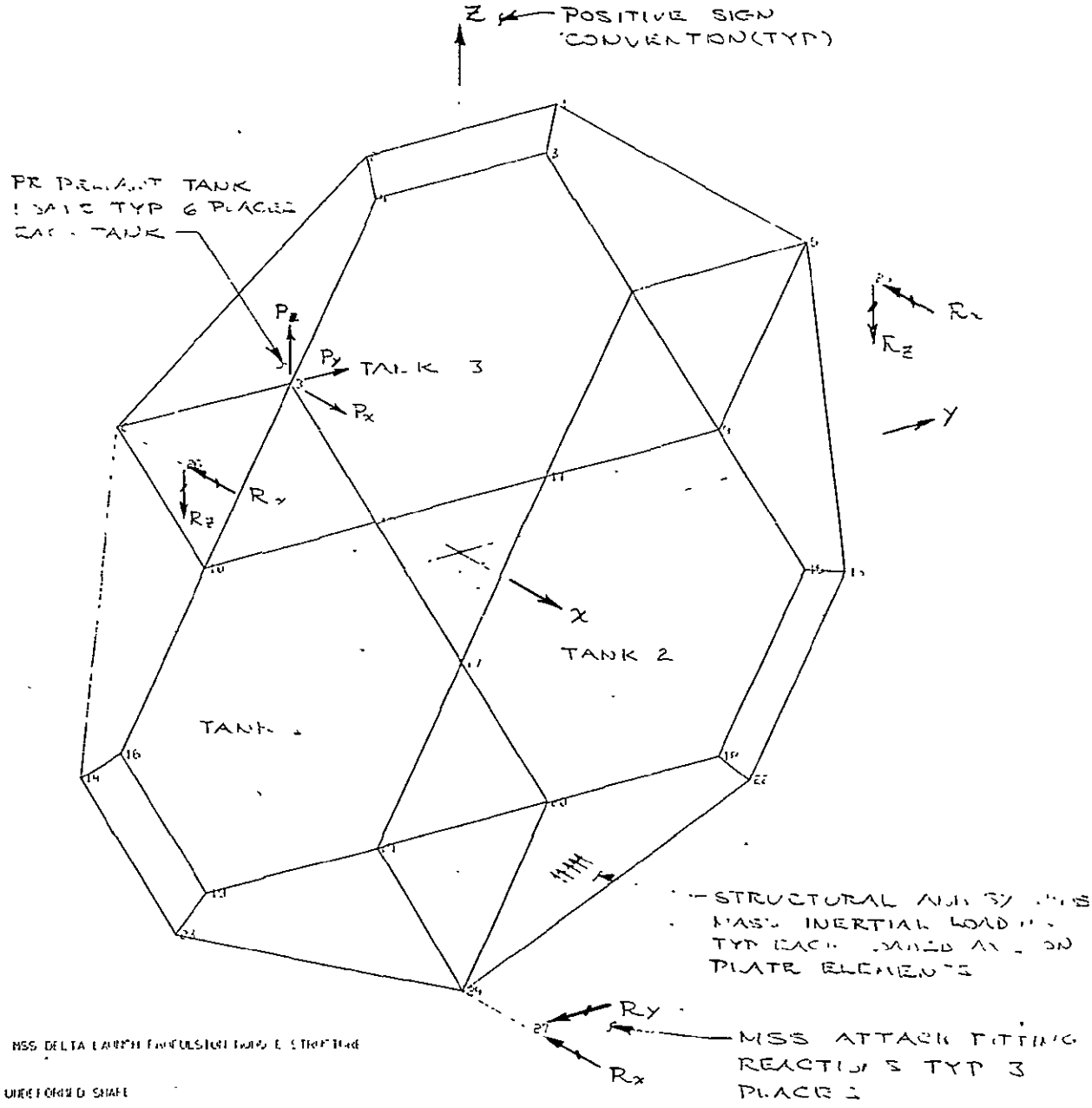

Figure 10. Structural Model Load/Reaction System

Table 2. Delta Propulsion Module Sizing Analysis Summary

ITEM	VALUE	NODE PT/ ELEMENT	NO. OF PROP TANKS	VEHICLE FLIGHT CONDITION
MAX. BAR ELEMENT TENSION	10,998 PSI	ELM. 68	2	DELTA POGO
MAX. BAR ELEMENT COMPRESSION	-11,811 PSI	ELM. 68	2	DELTA POGO
MAX. PLATE ELEMENT TENSION	9,726 PSI	ELM. 10	3	DELTA POGO
MAX. PLATE ELEMENT COMPRESSION	-11,408 PSI	ELM. 9	3	DELTA POGO
MAX. PLATE ELEMENT SHEAR	6,186 PSI	ELM. 9	3	DELTA POGO
MAX. Rx	2,007 LBS.	ND. 27	3	DELTA POGO
MAX. Ry	1,024 LBS	ND. 27	3	DELTA POGO
MAX. Rz	1,410 LBS	ND. 25	3	ORBITER LANDING
MAX. X AXIS DEFLECTION	-.117 IN.	ND.23	2	DELTA POGO
MAX. Y AXIS DEFLECTION	.107 IN.	ND.26	2	DELTA POGO
MAX. Z AXIS DEFLECTION	.069 IN.	ND. 27	2	DELTA POGO

NOTE: DELTA LOADS ARE YIELD AND ORBITER LOADS ARE ULTIMATE

Table 3. Mass Properties Summary - Spacecraft Propulsion Subsystem-I

Configuration	Weight (lb)	Center of Gravity (in.)			Moment of Inertia (slug ft^2)			Product of Inertia (slug ft^2)		
		x	y	z	I_x	I_y	I_z	I_{xy}	I_{xz}	I_{yz}
SPS-I (Two Tank Version)										
Structure	49.7	566.4	0.0	1.2	4.8	1.6	1.8	0	0	0
Propulsion System (wet)	122.8	567.6	-1.6	-4.2	7.3	1.6	6.1	0.2	0.1	0.5
Electrical and Electronic	44.0	566.0	-0.4	1.8	2.4	1.5	1.2	0	0	0
Total Module (wet)	216.5	567.0	-1.0	-1.8	14.8	5.1	9.1	0.1	-0.1	0.7
Less Expendables										
Propellant	-64.0	567.0	0.0	-5.2	-1.2	0	-1.2	0	0	0
Total, Module (dry)	152.5	567.0	-1.4	-0.3	13.4	4.9	7.9	0.1	-0.1	0.7
SPS-I (Three-Tank Version)										
Add										
Tank	12.2	567.0	0.0	10.8	-	-	-	-	-	-
Total Three-Tank Version (dry)	164.7	567.0	-1.3	0.5	-	-	-	-	-	-
Plus Expendables										
Propellant Upper Center	55.7	567.0	0.0	10.8						
Propellant Lower Left	55.7	567.0	-9.2	-5.2						
Propellant Lower Right	55.7	567.0	9.2	5.2						
Total, Three-Tank Version (wet)	331.8	567.0	-0.6	0.3	-	-	-	-	-	-

Table 4. Mass Properties Computer Printout - Two Task SPS-I

LANDSAT FOLLOW-ON,(SHORT PROP MODIS/A PCS A (9-3-76)

CP CODE	DESCRIPTION	WEIGHT POUNDS	S M	CENTER OF GRAVITY X (IN)	Y (IN)	Z (IN)	SH FA	A X	MOMENTS OF INERTIA X SLUG-FT2	Y SLUG-FT2	Z SLUG-FT2	REG X STA (IN)
PROPULSION MODULE (SHORT) SPS-1 DWG 42623-3 TWO TANK VERSION												
STRUCTURE												
0 0	BULKHEAD	24.2	0	567.8	500.0	500.0	22		3.3	0.9	0.9	0.
0 0	SUPPORT FTG (LOWER)	0.9	C	564.8	500.0	484.0	20		0.0	0.0	0.0	0.
0 0	SUPPORT FTG (UPR LH)	0.9	C	566.2	482.0	512.8	20		0.0	0.0	0.0	0.
0 0	SUPPORT FTG (UPR RH)	0.9	C	566.2	518.0	512.8	20		0.0	0.0	0.0	0.
0 0	UPPER ATT LATCH FTG (LH)	3.0	C	563.0	482.0	512.8	20		0.0	0.0	0.0	0.
0 0	UPPER ATT LATCH FTG (RH)	3.0	C	563.0	518.0	512.8	20		0.0	0.0	0.0	0.
0 0	LOWER ATTACH BRACKET	2.3	C	563.8	500.0	483.6	20		0.0	0.0	0.0	0.
0 0	LOWER ATT LATCH	1.0	C	559.6	500.0	484.0	20		0.0	0.0	0.0	0.
0 0	UPPER ELECTRONIC BRKT	1.7	C	562.2	486.4	508.0	20		0.0	0.0	0.0	0.
0 0	UPPER ELECTRONIC BRKT	1.7	C	562.2	513.6	508.0	20		0.0	0.0	0.0	0.
0 0	HEAT SHIELD	5.7	C	568.3	500.0	500.0	20		0.3	0.1	0.1	0.
1 0	MISC INSERTS & CONTINGEN	4.4	C	567.8	500.0	500.0	20		0.0	0.0	0.0	0.
TOTAL STRUCTURE (SHORT MODULE)												
	* FIRST LEVEL TOTAL	49.7		566.4	500.0	501.2			4.8 0.0	1.6 -0.0	1.8 -0.0	

Table 4. Mass Properties Computer Printout - Two Task SPS-I (Cont)

LANDSAT FOLLOW-ON,(SHORT PROP MOD)S/A PCS A (9-3-76)

OP CODE	DESCRIPTION	WEIGHT POUNDS	S M	CENTER OF GRAVITY X (IN)	Y (IN)	Z (IN)	SH FA	A X	MOMENTS OF INERTIA X SLUG-FT2	Y SLUG-FT2	Z SLUG-FT2	BEG X STA (IN)
ELECTRICAL & ELECTRONICS												
0 0	REMOTE INTERFACE UNIT	5.0	C	562.2	511.2	508.0	20		0.0	0.0	0.0	0.
0 0	REMOTE INTERFACE UNIT	5.0	C	562.2	488.8	508.0	20		0.0	0.0	0.0	0.
0 0	PMIU	3.5	C	564.0	500.0	521.2	20		0.0	0.0	0.0	0.
0 0	PMIU	3.5	C	572.1	489.6	517.6	20		0.0	0.0	0.0	0.
0 0	PMIU	3.5	C	572.1	518.0	510.4	20		0.0	0.0	0.0	0.
0 0	PMIU	3.5	C	572.1	510.4	482.0	20		0.0	0.0	0.0	0.
0 0	PMIU	3.5	C	572.1	477.5	489.6	20		0.0	0.0	0.0	0.
0 0	MAIN CONNECTOR	5.0	C	563.0	500.0	485.2	20		0.0	0.0	0.0	0.
4 0	WIRING	11.5	C	563.8	500.0	500.0	20		0.0	0.0	0.0	0.
TOTAL,ELECT & ELECTRONIC												
TOTAL PROPULSION MODULE (WET)												
	* FIRST LEVEL TOTAL	44.0		566.0	499.6	501.8			2.4 -0.0	1.5 -0.1	1.2 0.0	
	* SECOND LEVEL TOTAL	216.5		567.0	499.0	498.2			14.8 0.1	5.1 -0.1	9.1 0.7	
	* THIRD LEVEL TOTAL	216.5		567.0	499.0	498.2			14.8 0.1	5.1 -0.1	9.1 0.7	

Table 4. Mass Properties Computer Printout - Two Task SPS-I (Cont)

LANDSAT FOLLOW-ON,(SHORT PROP MOD)S/A PCS A (9-3-76)

OP CODE	DESCRIPTION	WEIGHT POUNDS	S M	CENTER OF GRAVITY X (IN)	Y (IN)	Z (IN)	SH FA	A X	MOMENTS OF INERTIA X SLUG-FT2	Y SLUG-FT2	Z SLUG-FT2	BEG X STA (IN)
PROPULSION SYSTEM (SHORT MOD)												
0 0	TANK (LH)	12.2	0	567.0	490.8	494.8	20		0.1	0.1	0.1	0.
0 0	TANK (RH)	12.2	0	567.0	509.2	494.8	20		0.1	0.1	0.1	0.
0 0	THRUSTER MODULE (ULH)	4.7	C	571.3	489.2	518.8	20		0.0	0.0	0.0	0.
0 0	THRUSTER MODULE (URH)	4.7	C	571.3	519.0	510.4	20		0.0	0.0	0.0	0.
0 0	THRUSTER MODULE (LLH)	4.7	C	571.3	482.0	489.2	20		0.0	0.0	0.0	0.
0 0	THRUSTER MODULE (LRH)	4.7	C	571.3	510.4	482.0	20		0.0	0.0	0.0	0.
0 0	LATCH VALVES (LH) 3	1.9	0	563.9	489.4	482.4	20		0.0	0.0	0.0	0.
0 0	LATCH VALVES (RH) 3	1.9	0	563.9	410.6	482.4	20		0.0	0.0	0.0	0.
0 0	FILTER	0.3	C	567.8	500.0	500.0	20		0.0	0.0	0.0	0.
0 0	FILL/DRAIN,GN2	0.3	0	565.4	490.0	520.4	20		0.0	0.0	0.0	0.
0 0	FILL/DRAIN,PROP	0.3	0	565.4	492.4	520.4	20		0.0	0.0	0.0	0.
0 0	PRESS TRANSDUCER	0.5	C	565.4	484.8	486.0	20		0.0	0.0	0.0	0.
0 0	TEMP TRANSDUCER (3)	1.5	C	565.4	500.0	500.0	20		0.0	0.0	0.0	0.
0 0	PLUMBING	3.0	0	566.0	500.0	500.0	20		0.0	0.0	0.0	0.
0 0	SUPPORTS	3.0	C	568.0	500.0	500.0	20		0.0	0.0	0.0	0.
0 0	PROPELLANT,RH TANK	32.0	C	567.0	509.2	494.8	20		0.0	0.0	0.0	0.
0 0	PROPELLANT,LH TANK	32.0	C	567.0	490.8	494.8	20		0.0	0.0	0.0	0.
1 0	CONTINGENCY	3.0	0	567.8	500.0	500.0	20		0.0	0.0	0.0	0.
TOTAL PROPULSION SYSTEM (NET)												
	* FIRST LEVEL TOTAL	122.8		567.6	498.4	495.8			7.3 0.2	1.6 0.1	6.1 0.5	

Table 4. Mass Properties Computer Printout - Two Task SPS-I (Cont)

LANDSAT FOLLOW-ON,(SHCR) PROP MODULE/A PCS A (9-3-76)

CP CODE	DESCRIPTION	WEIGHT POUNDS	S M	CENTER OF GRAVITY X (IN)	Y (IN)	Z (IN)	SH FA	A X	MOMENTS OF INERTIA X SLUG-FT2	Y SLUG-FT2	Z SLUG-FT2	REG X STA (IN)
LESS EXPENDABLES												
0 0	PROPELLANT,RH TANK	-32.0	0	567.0	509.2	494.8	20		0.0	0.0	0.0	0.
5 0	PROPELLANT,LH TANK	-32.0	0	567.0	490.8	494.8	20		0.0	0.0	0.0	0.
TOTAL EXPENDABLES												
TOTAL,PROPULSION MODULE (DRY)												
	* FIRST LEVEL TOTAL	-64.0		567.0	500.0	494.8			-1.2 0.0	0.0 0.0	-1.2 0.0	
	* SECOND LEVEL TOTAL	-64.0		567.0	500.0	494.8			-1.2 0.0	0.0 0.0	-1.2 0.0	
	* THIRD LEVEL TOTAL	152.5		567.0	498.6	499.7			13.4 0.1	4.9 -0.1	7.9 0.7	

The SPS-I utilizes three of the modified TIP-2 tanks to provide a maximum propellant capacity of 167.1 pounds at a 3:1 blowdown ratio. Increased propellant capacity can be obtained by accepting a larger blow-down ratio or by adding supplementary ullage volume in another tank. The upper limit for the selected tanks is 213.3 pounds which is set by the point at which the diaphragm is snug but not stretched. To maintain the 3:1 blow-down at this loading requires the addition of approximately 1800-cu.in. of ullage volume. Figures 11 and 12 show the schematic and design concept for this maximum capacity option utilizing a PSI tank developed for the Marots program for the ullage volume. The Marots tanks extends into the central volume of the MMS which would make this configuration incompatible with the standard on-orbit module exchange process. If subsequent mission analyses indicate the desirability of carrying this much propellant on a serviceable mission, it is possible that a special procedure could be derived to exchange this module since clearance exists around the Marots tank to permit some lateral motion for disengagement prior to lowering the module to clear the spacecraft structure.

3.3 SPS-IA DESIGN CONFIGURATIONS

For those missions of the MMS which do not require servicing but do need the maximum propellant capacity within the overall length constraints imposed by the launch vehicle adaptor, a propulsion module designated SPS-IA was derived. Figure 13 shows the schematic for this concept and Drawing 42623-5 illustrates the design concept. The system schematic is identical to the SPS-I except that two HEAO tanks modified to a 4:1 burst to operating pressure are added. This modification is estimated to increase the weight per tank to 19.5 pounds.

The HEAO tanks are mounted in the central volume of the MMS utilizing a cylindrical connection between the two tanks. This, in turn, is supported by three built-up structures which bridge to the spacecraft main longerons. The installation concept is that the tank support structures would be installed as part of the MMS structure build-up while the two HEAO tanks would be integrated with the rest of the SPS-IA system utilizing a piece of GSE to hold them in position. When the propulsion module was installed the HEAO tanks would be slipped into the central cavity concurrently with the attachment of the rest

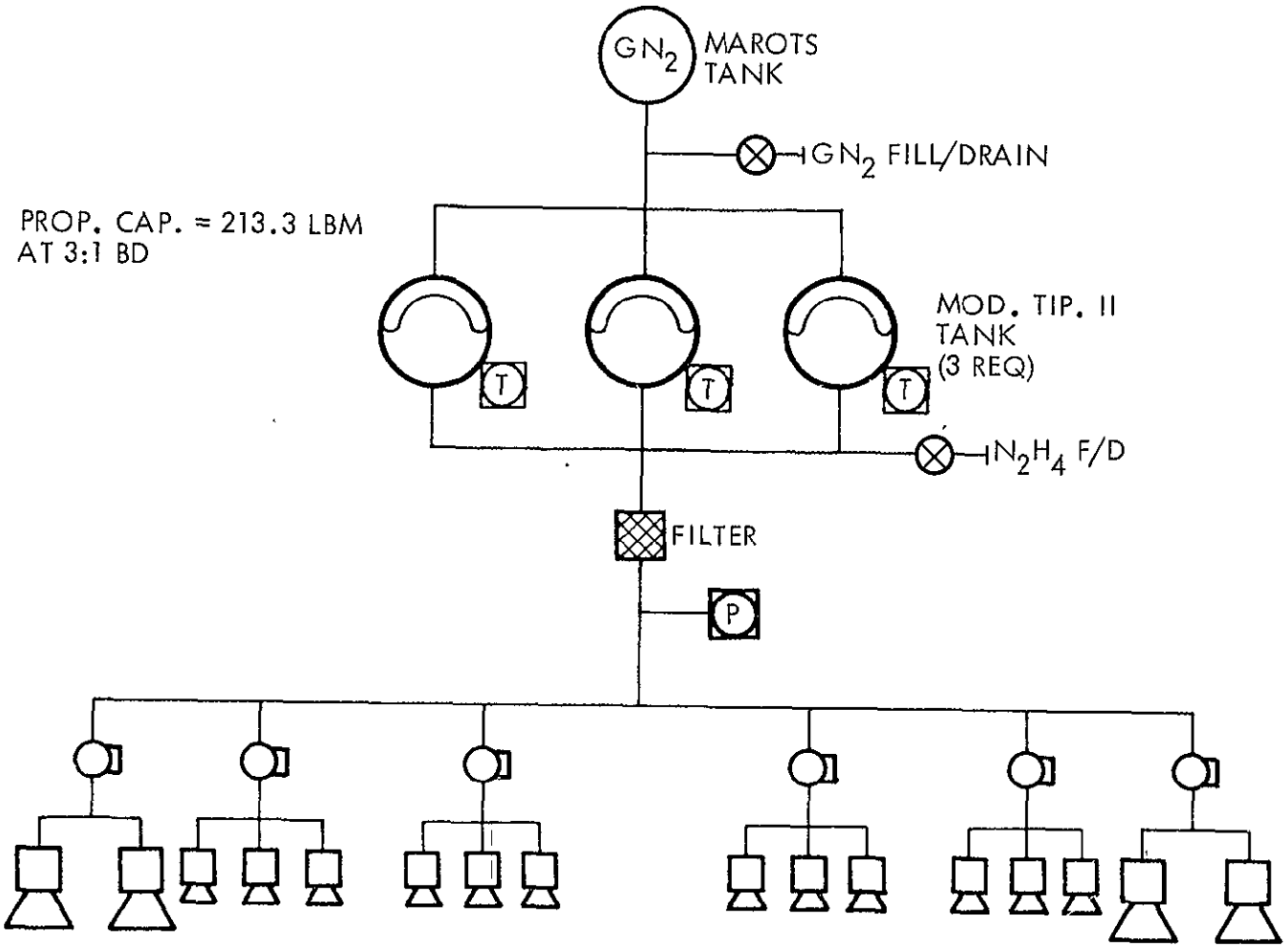

Figure 11. Maximum Capacity Version of SPS-I, Schematic

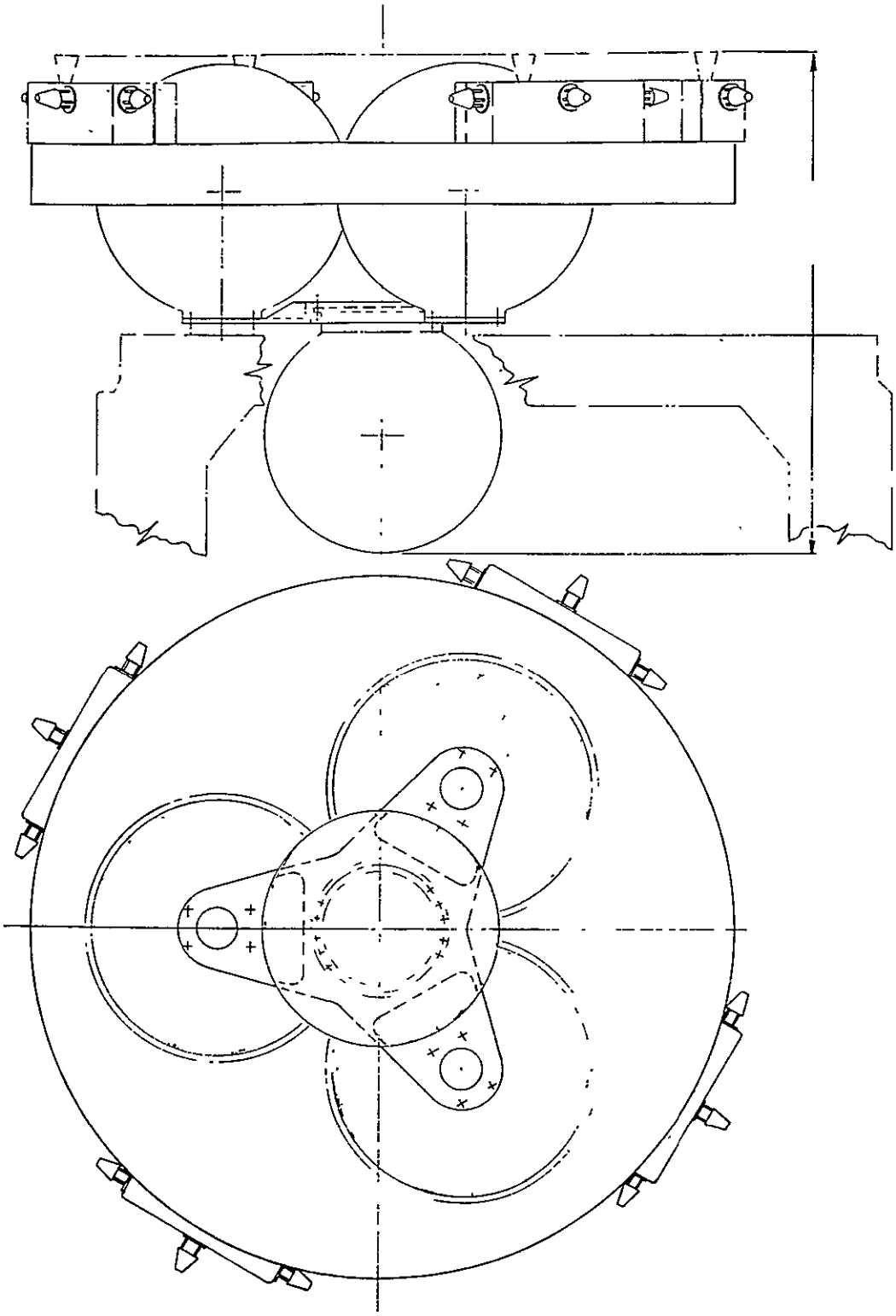

Figure 12. Maximum Capacity Version of SPS-1, Design Concept

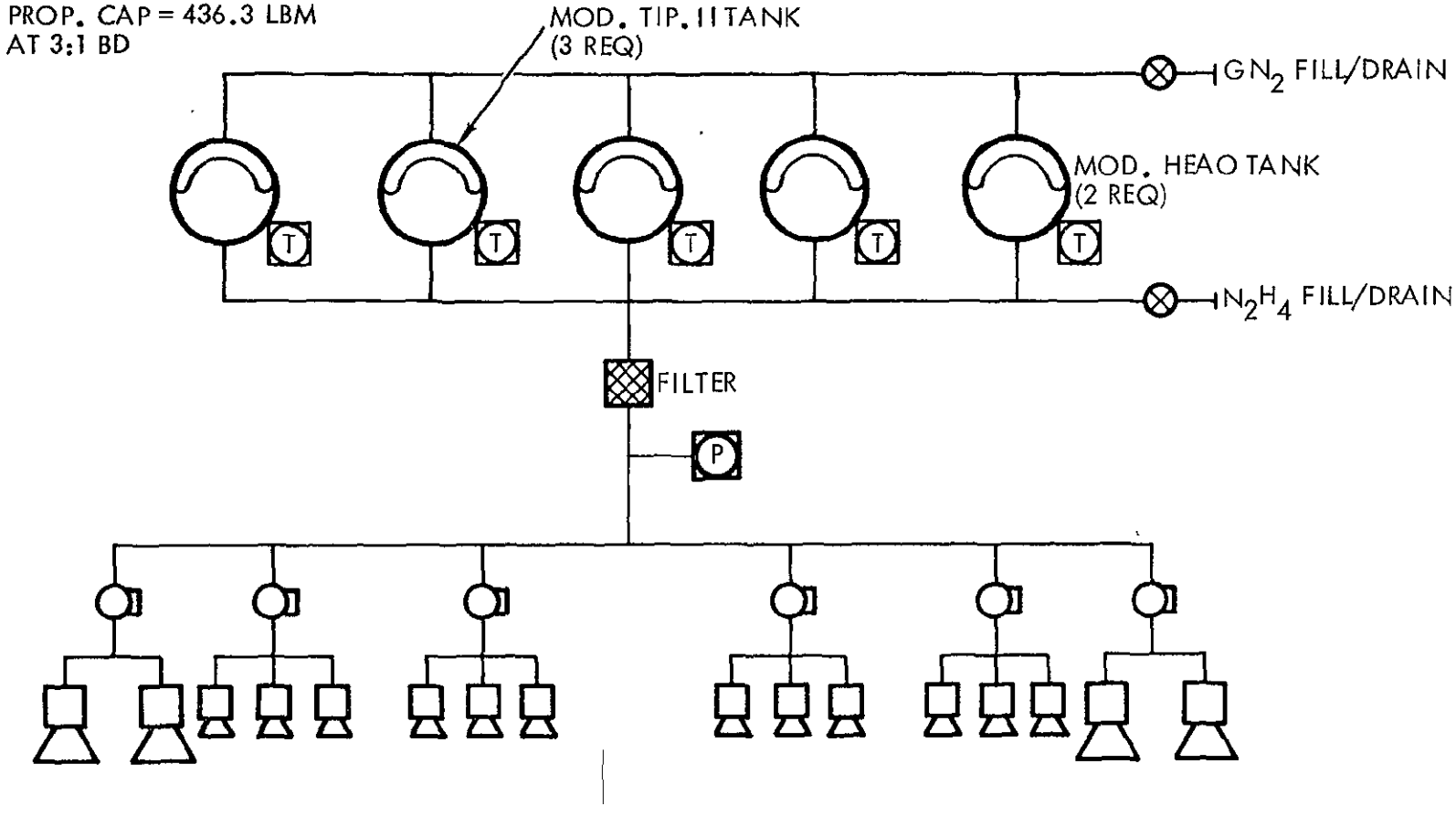

Figure 13. SPS-IA Propulsion Module Schematic

of the system to modified brackets on the aft face of the MMS. Brackets on the cylindrical interconnect between the two tanks would connect with the tank support structures and the support GSE could be removed. It should be noted that the electrical connection has to be performed as a separate operation after structural mating.

This system provides a total capacity of 436.3 pounds of hydrazine at a 3:1 blow-down ratio. No structural interferences were discovered with either the spacecraft structure or the module electrical connectors. There would be a significant impact on the thermal relationships between the various spacecraft elements, but this was not analyzed.

4.0 SHUTTLE MISSION CONFIGURATION

4.1 REQUIREMENTS

The propellant requirements for the mission where the spacecraft is delivered to orbit by the Shuttle, was determined by the analyses in Volume I to be 1027.6 pounds. This was based on a conservative analysis of the propellant required to transfer from a Shuttle-delivery orbit of 150-nmi to the operational orbit at 380.6 nmi, perform the same orbital functions required of the Delta-launched version, transfer back to the 150-nmi orbit for Shuttle retrieval or service, and provide control authority during the transfers.

The constraints on this design were not as severe as those for SPS-I in that there was no defined length limit. However, it was shown in Volume I that the present Shuttle cost share formulae places considerable emphasis on reducing the overall length of the payload. The constraints due to the module exchange process were the same, and the design was driven by the solutions found there in order to maintain a compatible interface with the MMS design and the MEM.

4.2 SPS-II DESIGN CONFIGURATION

It was decided to utilize existing tank designs to minimize development costs and the only viable candidate for this propellant quantity was found to be the Viking Orbiter '75 (VO '75) tank. As discussed in Volume I, this tank system utilizes a capillary propellant management device (PMD) to prevent uncovering of the propellant exit in zero-g. While there is some uncertainty about the compatibility of this device with the fuel and mission profile of the Landsat Follow-on/MMS, available data indicate that, pending definitive test, it appears to be an acceptable choice for the SPS-II propulsion module. A somewhat modified version of the VO '75 tank was utilized in that the burst to operating pressure was raised to 4:1 by increasing the wall thickness and the mounting fittings were changed (simplified) to better match the SPS-II configuration. The new tank weight was estimated to be 139 pounds without the PMD.

Figure 14 is the schematic for the SPS-II. It is identical to the SPS-I and -IA schematics except for the tankage. Drawing 42623-4 and Figure 15 and 16 illustrate the design concept. The basic structural approach involves the attachment of two ring structures to the VO '75 tank flanges. The forward ring provides the mounting plane for the module attachment brackets and the electrical connector which are identical to those on the SPS-I. The aft ring supports the REM's, control and monitoring electronics, and other system elements which also are identical to those on SPS-I. Since these elements are exposed to the plume back wash during the long orbit transfer burns, a heat shield covering everything except the REM's was included. Electrical connection between the front and back is carried through two wire tunnels.

Because of its length (~60 inches) and weight (~1500 pounds) the SPS-II could require lateral load support to the Flight Support System (FSS). The support concept considered is shown in line diagram in Figure 17. Two support struts are considered as shown in order to react loads in any lateral axis as well as avoid interference with the lower arm of the FSS berthing cage. Dynamic studies conducted to date have shown orbiter liftoff conditions generate Y axis loads nearly as severe as the Z axis loads of the landing conditions. Therefore, a support system with the capability of reacting loads in any lateral axis may be required.

It should be noted that the lateral load supports will be required only if the moment relief supplied by connecting the berthing cage to the MMS is insufficient. Additional moment relief could be achieved if a new propellant tank were designed for the SPS-II such that the overall length was reduced to approximately 30 inches. This additional moment relief would reduce the possible requirement for lateral load supports appreciably. Interface loads at the MMS latches for the orbiter landing condition resulting from static analysis are shown in Table 5 for these various concepts to illustrate this point. The SPS load/reaction system is shown in Figure 18. It should also be noted that the preliminary analysis of Shuttle transportation costs in Volume I indicated a potential gain by designing a unique tank which would shorten the overall payload length.

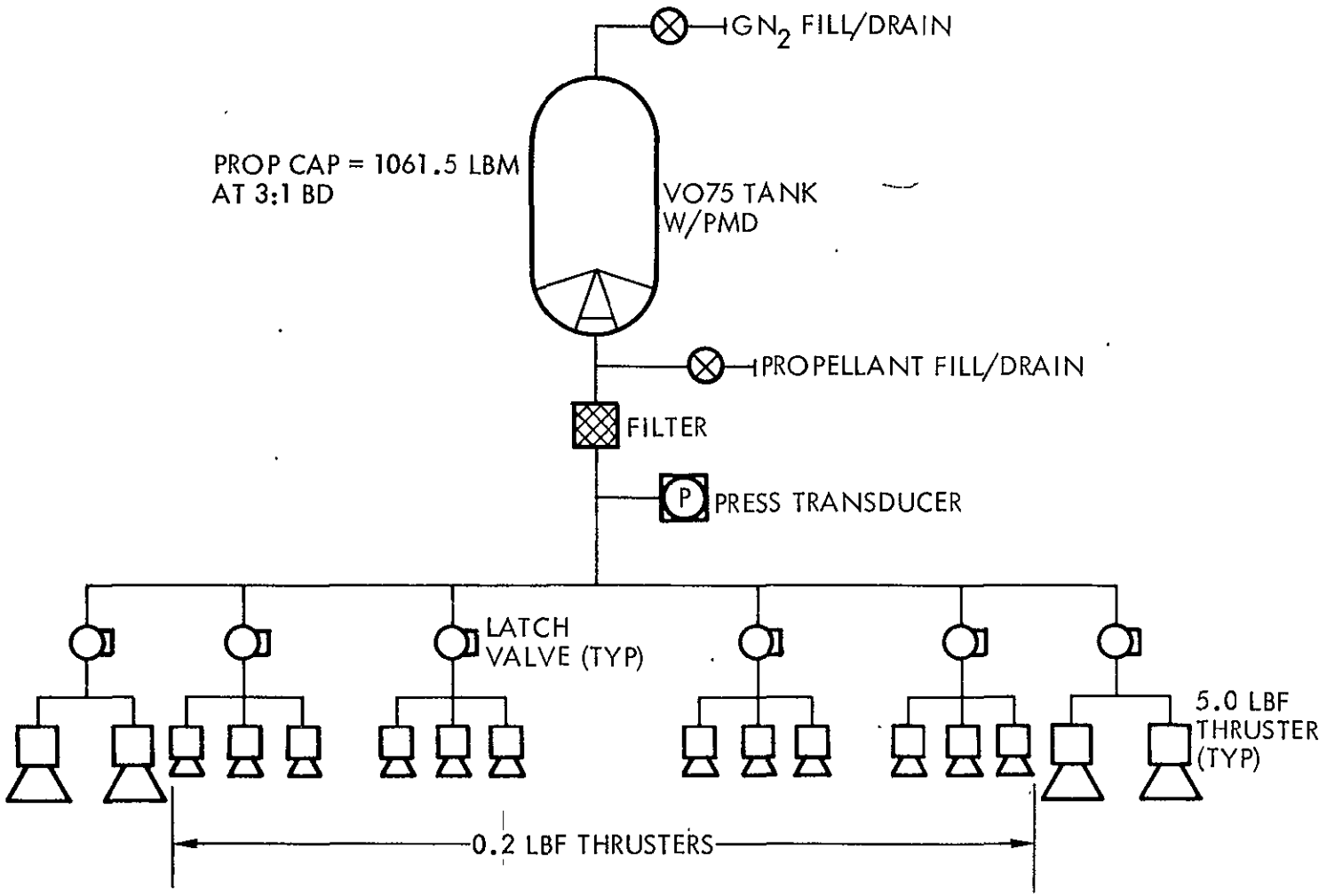

Figure 14. SPS-II Propulsion Module Schematic

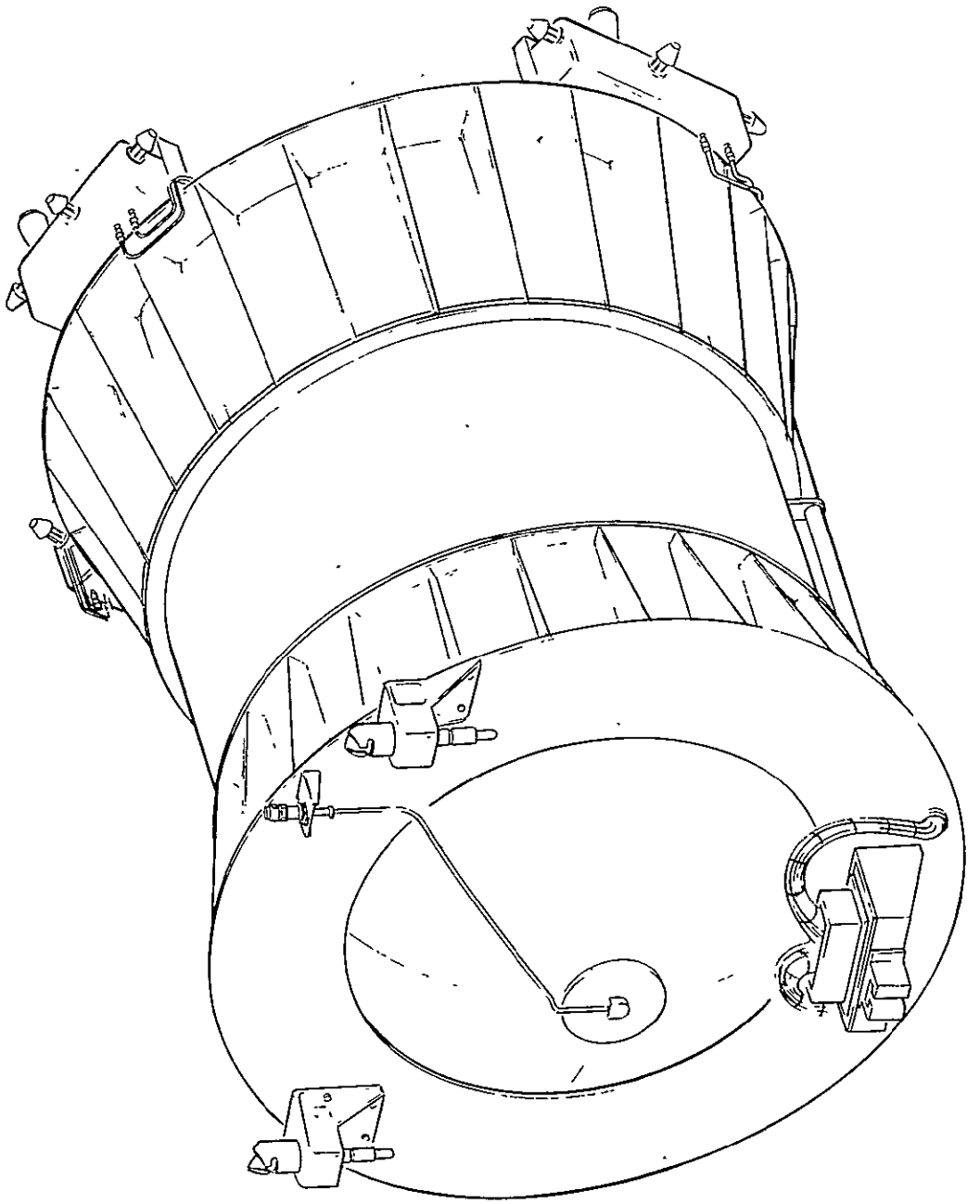

Figure 15. SPS-II Perspective

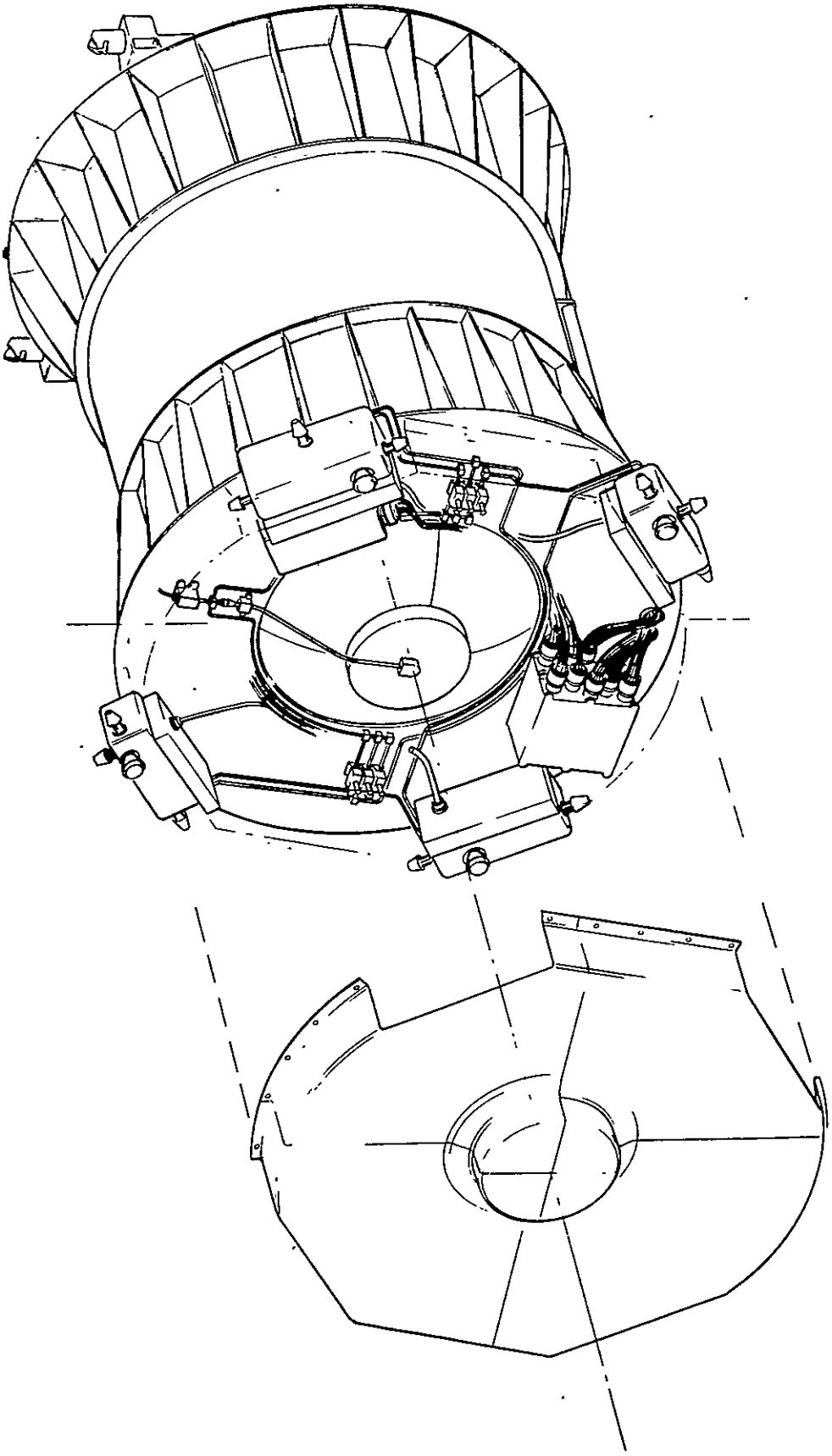

Figure 16. SPS-II Perspective, Aft View

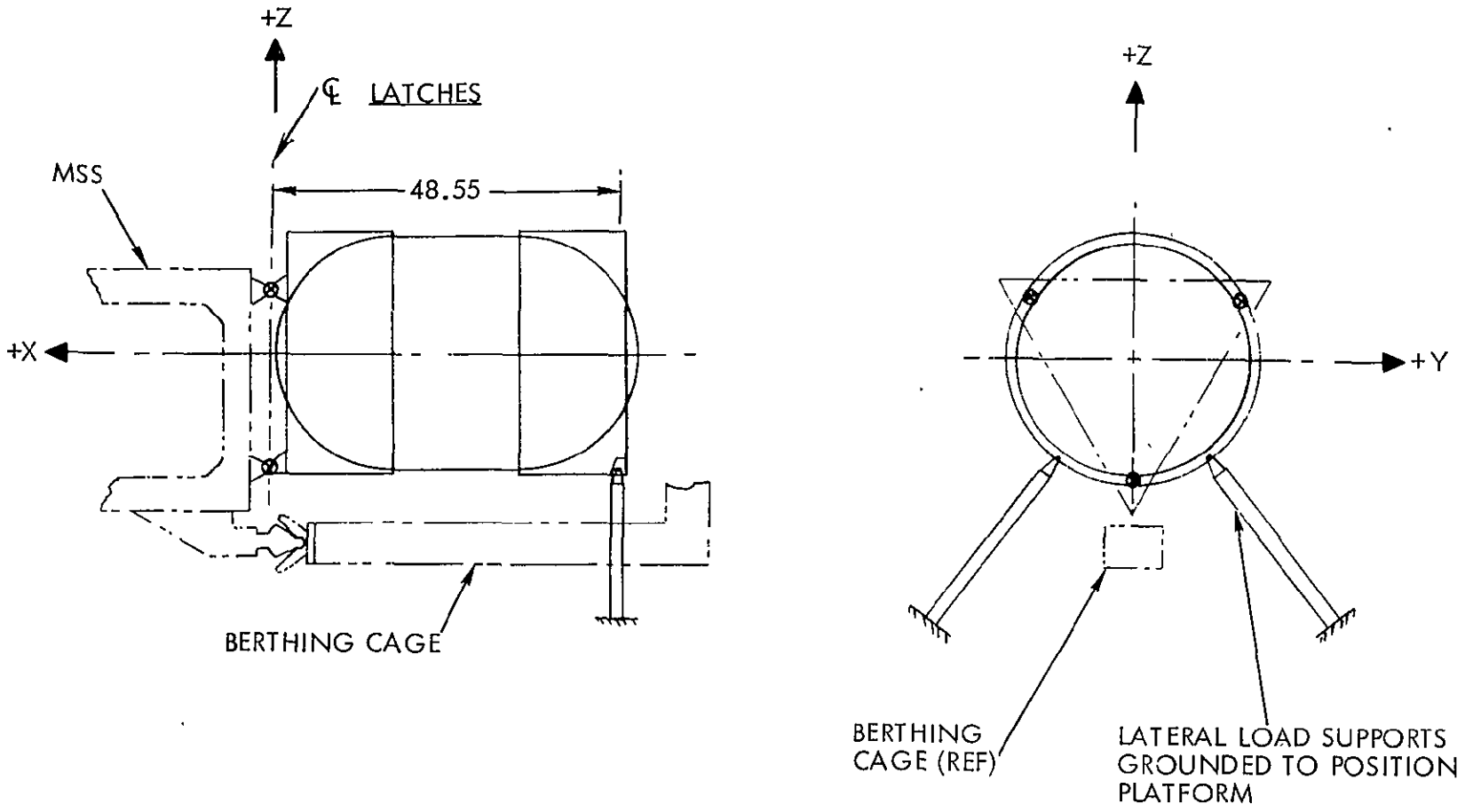

Figure 17. SPS-II Lateral Load Support Concept

Table 5. SPS-II/MSS Interface Loads

SPS-II Concept	Max. Latch Reactions~Lbs		
	R_x	R_y	R_z
Baseline SPS-II without lateral load supports	9,775	3,300	6,750
Baseline SPS-II with lateral load supports	2,090	1,650	5,175
30 inch SPS-II without lateral load supports	5,860	3,300	6,005

Estimated mass properties for the SPS-II configuration are summarized in Table 6 and shown in detail in the computer printout (Table 7). As indicated for the SPS-I mass-properties print-out, there is a 500-in. bias inserted in the y- and z- center of gravity figures which has been removed in Table 6.

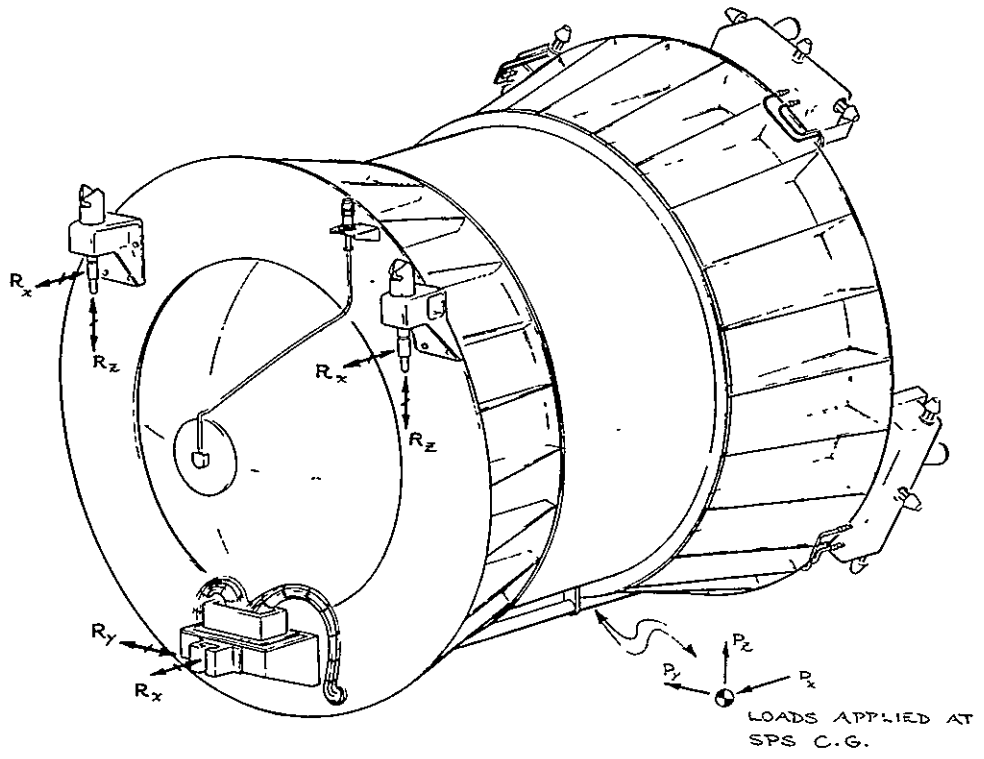

Figure 18. SPS-II Load/Reaction System

Table 6. Mass Properties Summary - Spacecraft Propulsion System-II

SPS II	Weight (lb)	Center of Gravity (in.)			Moment of Inertia (slug-ft^2)			Product of Inertia (slug-ft^2)		
		X	Y	Z	I_X	I_Y	I_Z	I_{XY}	I_{XZ}	I_{YZ}
Structure	48.0	582.5	0.2	0.2	3.3	7.3	7.3	0.1	-0.1	0.1
Propulsion System (wet)	1241.8	588.4	0.0	0.0	8.7	17.5	17.6	0	0.1	0
Electrical Electronic	63.0	597.0	-0.4	-9.5	2.3	6.0	5.4	-0.1	0.9	0.3
Total, Module (wet)	1352.8	588.5	0.0	-0.4	15.5	33.4	31.7	-0.1	-0.3	0.4
Less Expandables Propellant	-1061.5	587.5	0.0	0.0	0	0	0	0	0	0
Total, Module (dry)	291.3	592.4	0.0	-2.0	15.3	32.0	30.5	0	0.2	0.4

Table 7. Mass Properties Computer Printout, SPS-II

LANDSAT FOLLOW-ON (LONG PROP.MOD) (9-17-74)

OP CODE	DESCRIPTION	WEIGHT POUNDS	S M	CENTER OF GRAVITY X (IN)	Y (IN)	Z (IN)	SH FA	A X	MOMENTS OF INERTIA X SLUG-FT2	Y SLUG-FT2	Z SLUG-FT2	BEG X STA (IN)
PROPULSION MODULE SPS II DWG 42623-4												
STRUCTURE												
0 0	FWD RING STRUCTURE	13.1	C	559.1	500.0	500.0	1	X	1.0	0.5	0.5	0.
0 0	AFT RING STRUCTURE	9.9	C	608.4	500.0	500.0	1	X	0.7	0.4	0.4	0.
0 0	SUPT FTG-LOWER	1.0	C	566.3	500.0	482.0	20		0.0	0.0	0.0	0.
0 0	SUPT FTG-(UPPER LH)	1.0	C	566.3	481.2	512.0	20		0.0	0.0	0.0	0.
0 0	SUPT FTG-(UPPER RH)	1.0	C	566.3	518.8	512.0	20		0.0	0.0	0.0	0.
0 0	UPR ATTACH LATCH FTG-LH	3.0	C	563.0	481.2	512.0	20		0.0	0.0	0.0	0.
0 0	UPR ATTACH LATCH FTG-RH	3.0	C	563.0	518.8	512.0	20		0.0	0.0	0.0	0.
0 0	LOWER ATTACH BRACKET	2.3	C	563.0	500.0	492.0	20		0.0	0.0	0.0	0.
0 0	LOWER ATTACH LATCH	1.0	C	563.0	500.0	482.0	20		0.0	0.0	0.0	0.
0 0	UPR ELECTRONIC BRKT	1.7	C	612.0	512.4	509.6	20		0.0	0.0	0.0	0.
0 0	UPR ELECTRONIC BRKT	1.7	C	612.0	493.6	484.0	20		0.0	0.0	0.0	0.
0 0	HEAT SHIELD	4.8	C	613.6	500.0	500.0	20		0.3	0.1	0.1	0.
1 0	CONTINGENCY	4.5	C	585.0	500.0	500.0	20		0.0	0.0	0.0	0.
TOTAL.STRUCTURE												
	* FIRST LEVEL.TOTAL	48.0		582.5	500.2	500.2			3.3 0.1	7.3 -0.1	7.3 0.1	

Table 7. Mass Properties Computer Printout, SPS-II (Cont)

LANDSAT FOLLOW-ON (LONG PROP.MOD) (9-17-76)

OP CODE	DESCRIPTION	WEIGHT POUNDS	S M	CENTER OF GRAVITY X (IN)	Y (IN)	Z (IN)	SH FA	A X	MOMENTS OF INERTIA X SLUG-FT2	Y SLUG-FT2	Z SLUG-FT2	REF X STA (IN)
PROPULSION SYSTEM												
0 0	TANK (VO-75)	139.0	C	587.5	500.0	500.0	3	X	6.4	10.8	10.8	0.
0 0	PROP MANAGEMENT SYST	7.8	C	614.0	500.0	500.0	20		0.0	0.0	0.0	0.
0 0	THRUSTER MODULE (LLH)	4.7	C	613.6	489.0	519.2	20		0.0	0.0	0.0	0.
0 0	THRUSTER MODULE (URH)	4.7	C	613.6	519.2	511.0	20		0.0	0.0	0.0	0.
0 0	THRUSTER MODULE (LLH)	4.7	C	613.6	511.2	481.2	20		0.0	0.0	0.0	0.
0 0	THRUSTER MODULE (LRH)	4.7	C	613.6	480.8	489.2	20		0.0	0.0	0.0	0.
0 0	LATCH VALVES (LH)(3)	1.9	C	612.0	486.0	504.0	20		0.0	0.0	0.0	0.
0 0	LATCH VALVES (RH)(3)	1.9	C	612.0	514.0	496.0	20		0.0	0.0	0.0	0.
0 0	FILTER	0.3	0	612.0	503.6	513.2	20		0.0	0.0	0.0	0.
0 0	FILL/DRAIN,GN2	0.3	C	612.0	503.6	513.2	20		0.0	0.0	0.0	0.
0 0	FILL/DRAIN,PROP.	0.3	C	612.0	503.6	513.2	20		0.0	0.0	0.0	0.
0 0	PRESS TRANSDUCER	0.5	C	612.0	505.2	519.2	20		0.0	0.0	0.0	0.
0 0	TEMP TRANSDUCER	0.5	C	612.0	500.0	500.0	20		0.0	0.0	0.0	0.
0 0	PLUMBING	3.0	C	612.5	500.0	500.0	20		0.0	0.0	0.0	0.
0 0	SUPPORTS	3.0	C	612.0	500.0	500.0	20		0.0	0.0	0.0	0.
0 0	PROPELLANT	1061.5	C	587.5	500.0	500.0	20		0.0	0.0	0.0	0.
1 C	CONTINGENCY	3.0	C	611.0	500.0	500.0	20		0.0	0.0	0.0	0.
TOTAL,PROPULSION SYST (WET)												
*	FIRST LEVEL TOTAL	1241.8		588.4	500.0	500.0			8.7 0.0	17.5 0.1	17.6 -0.0	

Table 7. Mass Properties Computer Printout, SPS-II (Cont)

LANDSAT FOLLOW-ON (LONG PROP.MOD) (9-17-76)

OP CODE	DESCRIPTION	WEIGHT POUNDS	S M	CENTER OF GRAVITY X (IN)	Y (IN)	Z (IN)	SH FA	A X	MOMENTS OF INERTIA X SLUG-FT2	Y SLUG-FT2	Z SLUG-FT2	BEG X STA (IN)
ELECTRICAL & ELECTRONICS												
0 0	REMOTE INTERFACE UNIT	5.0	C	614.0	493.2	483.6	20		0.0	0.0	0.0	0.
0 0	REMOTE INTERFACE UNIT	5.0	C	614.0	493.2	483.6	20		0.0	0.0	0.0	0.
0 0	PMIU	3.5	C	613.6	490.0	517.2	20		0.0	0.0	0.0	0.
0 0	PMIU	3.5	C	613.6	517.0	509.8	20		0.0	0.0	0.0	0.
0 0	PMIU	3.5	C	613.6	510.0	493.0	20		0.0	0.0	0.0	0.
0 0	PMIU	3.5	C	613.6	482.6	490.0	20		0.0	0.0	0.0	0.
0 0	PMIU	3.5	0	613.6	512.6	509.4	20		0.0	0.0	0.0	0.
0 0	MAIN CONNECTOR	5.0	C	563.0	500.0	485.6	20		0.0	0.0	0.0	0.
0 0	WIRING	25.0	C	587.5	500.0	485.0	1	X	0.0	1.1	1.1	0.
4 0	CONTINGENCY	5.5	C	587.5	500.0	496.0	20		0.0	0.0	0.0	0.
TOTAL,ELECTRICAL & ELECTRONIC												
TOTAL,PROPULSION MODULE (WET)												
	* FIRST LEVEL TOTAL	63.0		597.0	499.6	490.5			2.3 -0.1	6.0 0.9	5.4 0.3	
	* SECOND LEVEL TOTAL	1352.8		588.5	500.0	499.6			15.5 -0.1	33.4 -0.3	31.7 0.4	
	* THIRD LEVEL TOTAL	1352.8		588.5	500.0	499.6			15.5 -0.1	33.4 -0.3	31.7 0.4	

Table 7. Mass Properties Computer Printout, SPS-II (Cont)

LANDSAT FOLLOW-ON (LONG PROP.MOD) (9-17-76)

OP CODE	DESCRIPTION	WEIGHT POUNDS	S M	CENTER OF GRAVITY X (IN)	Y (IN)	Z (IN)	SH FA	A X	MOMENTS OF INERTIA X SLUG-FT2	Y SLUG-FT2	Z SLUG-FT2	BEG X STA (IN)
	LESS EXPENDABLES											
5 0	PROPELLANT	-1061.5	C	587.5	500.0	500.0	20		0.0	0.0	0.0	0.
	TOTAL EXPENDABLES											
	TOTAL PROPULSION MODULE (DRY)											
	* FIRST LEVEL TOTAL	-1061.5		587.5	500.0	500.0			0.0 0.0	0.0 0.0	0.0 0.0	
	* SECOND LEVEL TOTAL	-1061.5		587.5	500.0	500.0			0.0 0.0	0.0 0.0	0.0 0.0	
	* THIRD LEVEL TOTAL	291.3		562.4	500.0	498.0			15.3 -0.0	32.0 0.2	30.5 0.4	

5.0 ELECTRICAL CONTROL AND DATA HANDLING

The command and control concept mechnized on the MMS is one where all commands and information signals originate and terminate at central equipment. The MMS command and data handling subsystem (C&DH) performs this function with a computer serving as the centralized element and remote interface units (RIU) acting as the devices which distribute commands and signals from other MMS subsystems and experiments (see Figure 19).

The interface between the RIU and the subsystems has specific electrical characteristics, not generally compatible with the propulsion module (PM) electrical-mechanical components (propulsion jets tranducers, etc.). This RIU input/output necessitates additional equipment to adapt the RIU to the PM components, identified as a propulsion module interface unit (PMIU).

This section describes the requirements and concept mechanization of the equipment located in the PM to control the PM and handle the data originating there. Included is the mechanization of the PMIU and a description of its interfaces with the RIU and PM.

5.1 REQUIREMENTS

The functional requirements of the electrical control and data handling equipment in the PM are to:

1. Drive the solenoids in the thruster jets from command signals which are received from
   - The RIU.
   - The attitude control system (ACS) via hardwire (low-thrust jets only).
2. Drive the latch valves from command signals which are received from the RIU's.
3. Control the temperature of the thruster catalytic heaters.
4. Control the temperature of the PM components.

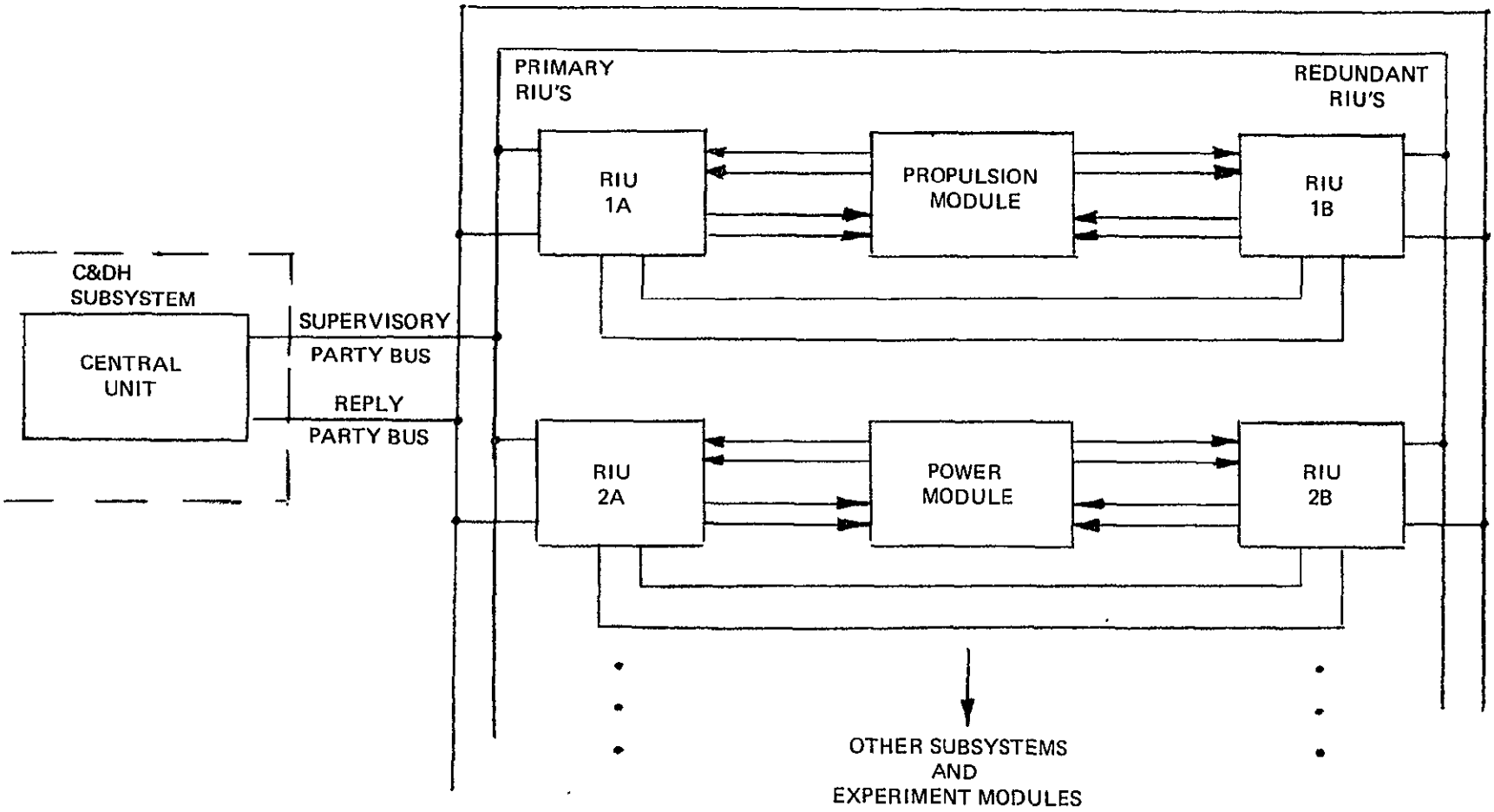

Figure 19. Block Diagram of CU-RIU Configuration

5. Provide PM performance data to the RIU and the PM interface connector with signal conditioning as required.

6. Route PM command signals and resulting performance status through an access connector for checkout purposes (not functionally required).

The electronics to control the PM include the RIU and the PMIU between the RIU and the PM components. These electronic packages must fit within the space available in the PM, which in turn is constrained by the MMS. Space is very critical in the Delta-launched PM (SPS-I); therefore, the electronics must be mechanized to conserve volume.

The jet thrusters are packaged in rocket engine modules. The REM's are placed around the PM to provide adequate X, Y, and Z control. Functionally an electronics package is required between the REM and RIU with the largest number of wires required between the REM and the electronics. This wiring is also the noisiest electrically since large currents are switched into inductive loads. To save weight (copper) and reduce the radiation effects, these electronics should be placed close to the REM's.

5.2 CONTROL CONCEPT

Three functional types of control are required to operate the PM: valve control (thrust and fluid), catalytic heater, and PM component temperature. In addition, signal conditioning is required to match the output of the transducers with the inputs to the RIU. The transducers provide the temperature and pressure status of the propellant in the tanks.

The concept for controlling the valves is shown by Figure 20. A signal from one or both of the redundant RIU's will be conditoned, stretched in time, and drive redundant relays, either of which will allow current to flow to the solenoid of the selected valve. Suppression is placed across all solenoids to reduce electrical noise.

The concept for controlling the catalytic heaters is shown by Figure 21. The sensor (t_o), measuring the catalytic bed temperature is one leg of a bridge. The bridge is excited at equally spaced time intervals by the RIU's Type IV constant-current output signal. The analog output of the bridge is fed into temperature "high-low" logic which in turn controls the application

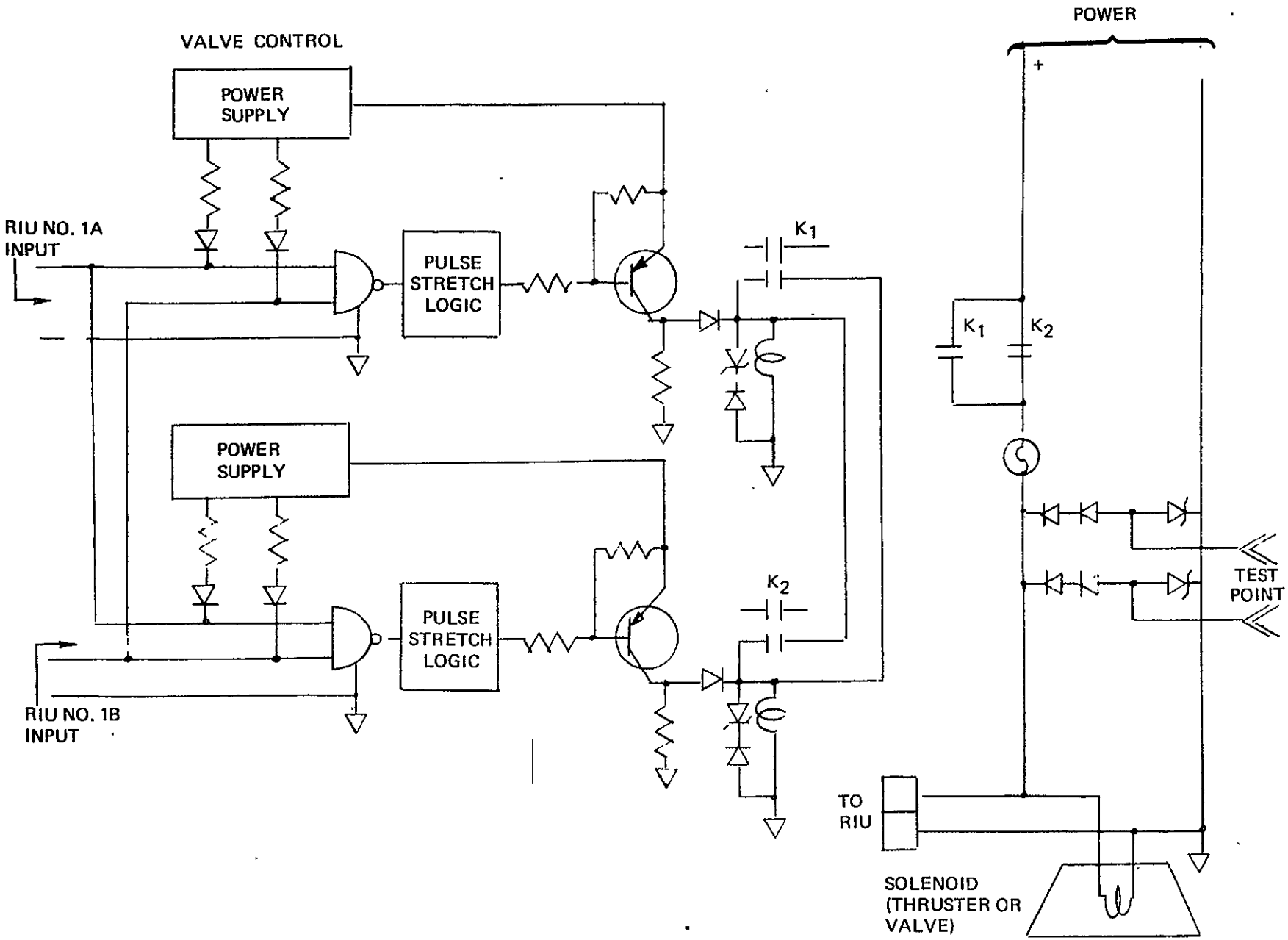

Figure 20. Propulsion Module Control Concept

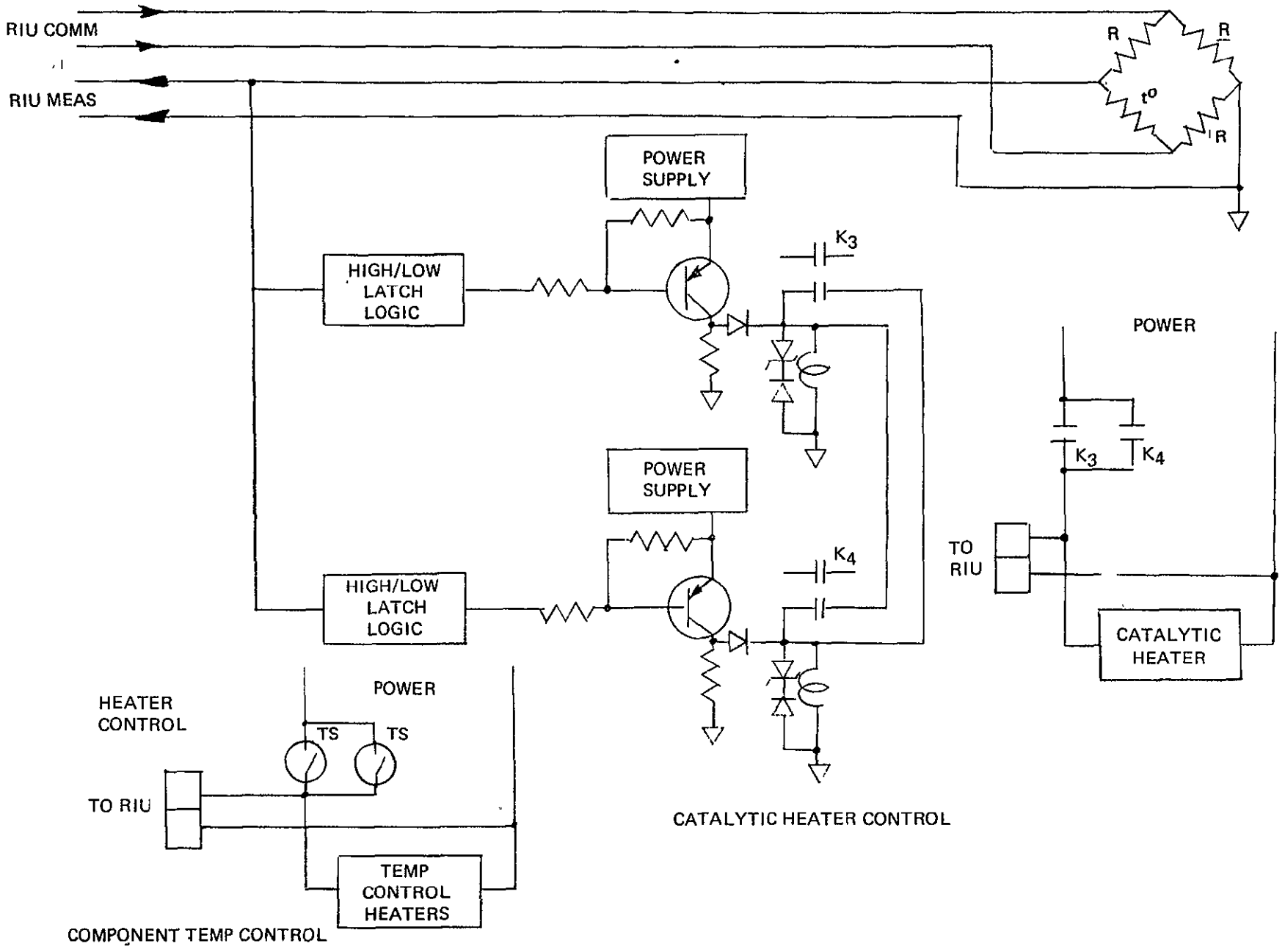

Figure 21. Temperature Control

of current to the heater elements. The circuitry is redundant from the analog temperature input through the relays applying current to the heaters.

The concept for controlling the temperature of the PM components consists of redundant temperature-sensitive switches applying current to heater strips secured to the component as shown by Figure 21.

To condition the signals from the transducer, normal signal conditioning techniques could be used. The transducers and sold-state amplifiers would periodically be supplied a power pulse from the RIU's Type IV constant-current output and the resulting conditioned transducer signal fed to an RIU input channel. Any caution and warning signals originating in the propulsion module are transmitted over hardwire from their initial source (with conditioning if required) to the module interface connector and, in turn, to the MMS umbilical and to the Shuttle.

The electronics required to accomplish the electrical control and data handling of the PM is defined as the RIU and PMIU. The RIU is supplied as part of the C&DH subsystem but the PMIU would be a specially built unit for the PM. The PMIU would contain all the special electrical functions described previously and is visualized to be packaged as five separate elements to minimize the wiring and EMI impact as previously discussed. Four of the PMIU's would be identical, each used to control one of the REM's. A fifth PMIU would contain the controls for the latch valves, signal conditioning, and circuitry for PM component temperature control. (Further study may show that all five PMIU's could be identical with the signal conditioning and component temperature control shared by each.)

Figure 22 shows in block diagram format the equipment and interfaces to control the PM. Physically each PMIU is placed right next to the REM with which it is associated, thus minimizing cable length. (Further study may show the desirability of making the PMIU a plug-in module of the REM.)

The interface wiring between PM components is shown in Table 8. The total wiring of a given component is shown in the Total column. The analysis which was performed to develop these data was made to size the connectors and estimate the weight and therefore cannot be directly related to the signals between components or RIU input/output selection.

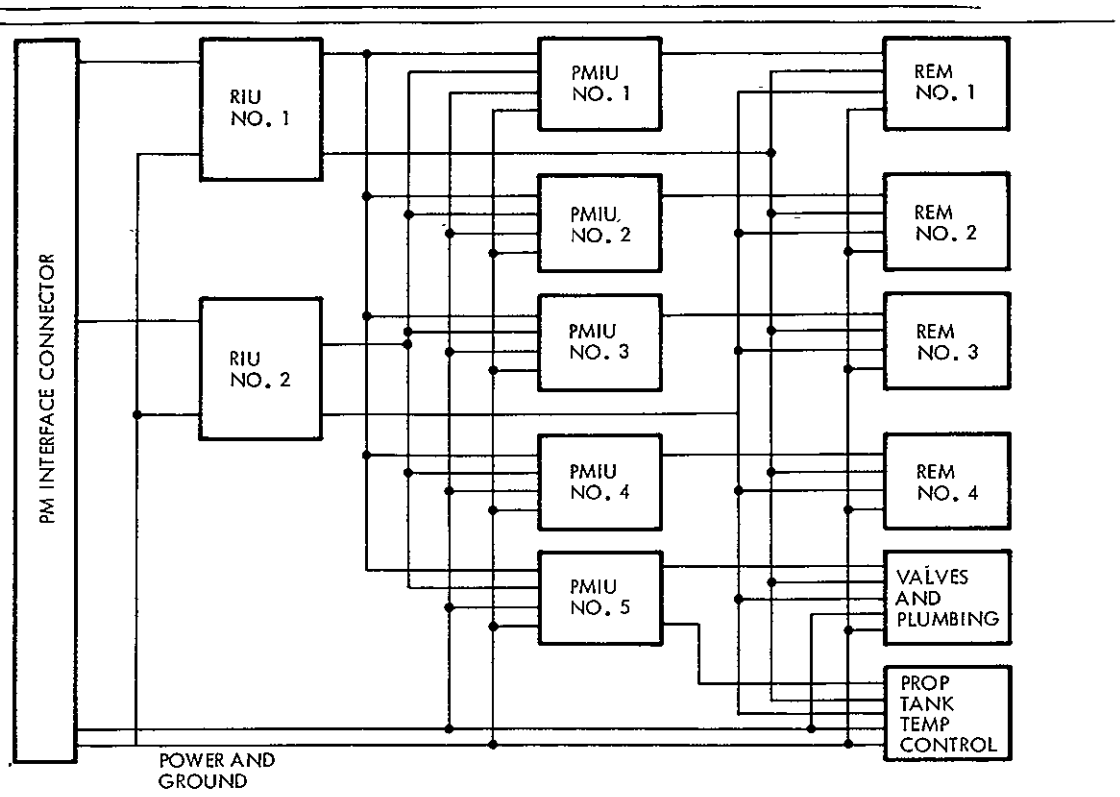

Figure 22. Propulsion Module Electrical Control and Data Handling

Table 8. Interface Wiring Wire Terminations Between PM Components

To → / From ↓	REM's 1-4	Valves and Plumbing	Prop Tank Temp. Cont	PMIU's 1-4	PMIU 5	RIU 1	RIU 2	PM Conn	Total
REM's 1-4 (each)				48		18	18	5	89
Valves and plumbing					24	12	12	5	53
Propellant tank temperature control					48	3	3	5	59
PMIU's 1-4 (each)	48					12	12	19	91
PMIU 5		24	48			12	12	25	121
RIU 1	72	12	3	48	12			10	172
RIU 2	72	12	3	48	12			10	172
PM Connector	—	40 total	—	—	—	—	—		40

The usage of the RIU input/output channels was not evaluated. A detailed analysis of the measurement and command type of signals required versus those available from the RIU must be made to assess the adequacy of one RIU to accomplish the electrical control and data handling function. The second RIU is to be redundant and must carry the same functions.

5.3 PHYSICAL CHARACTERISTICS

Physical characteristics are presented in Table 9 for the RIU, PMIU, and the wiring necessary to cable the equipment together. The RIU characteristics are taken directly from GSFC document S-714-11, Preliminary Specification for STACC Remote Interface Unit and Expander Unit. The PMIU and cabling were estimated. The estimates do not include the power necessary for thermal heaters.

Table 9. Physical Characteristics

Item	Unit Weight (lb)	Unit Volume ($in.^3$)	Avg. Power (watts)	Peak Power (watts)
RIU	5.0	140	∿1.5	5.6
PMIU's 1-4	3.5	82	2.1	3.7
PMIU 5	3.5	80	2.3	3.9
Cabling	11.36	-	-	-

6.0 PLUME ANALYSES

6.1 PLUME ENVELOPES

The plume envelopes resulting from an inviscid flow analysis are presented in this section. The coordinate system for the plume envelopes is presented in Figure 23. The exhaust plumes presented (Figures 24 through 30) depict space or flight conditions.

Because the plume envelopes were developed using an inviscid flow analysis, the outer portions of the plume are not necessarily valid. The gas in the viscous boundary layer within the nozzle will expand to much greater angles than predicted with an inviscid flow analysis. The portion of the flow area which is unaffected by the boundary layer is approximated by the following relationship:

$$F = \frac{(R_e - \delta)^2}{R_e^2} = 1 - 2\left(\frac{\delta}{R_e}\right) + \left(\frac{\delta}{R_e}\right)^2$$

where

F = Fraction of flow area unaffected by boundary layer

R_e = Nozzle exit plane radius, inches

δ = Boundary layer thickness of the nozzle exit plane, inches

Using the relationship developed in Reference 1, the following boundary layer thickness-to-nozzle exit radius ratios were determined:

Thruster	$\frac{\delta}{R_e}$	F
0.2-lbf	0.297	0.494
5 -lbf	0.179	0.674
100-lbf	0.105	0.801

Thus, for the 0.2-lbf thruster, gas flow between the 100 percent and 49.4 percent contours shown in Figure 24 will not be valid. Within this region, the flow expansion will be greater. The effect of the nozzle boundary

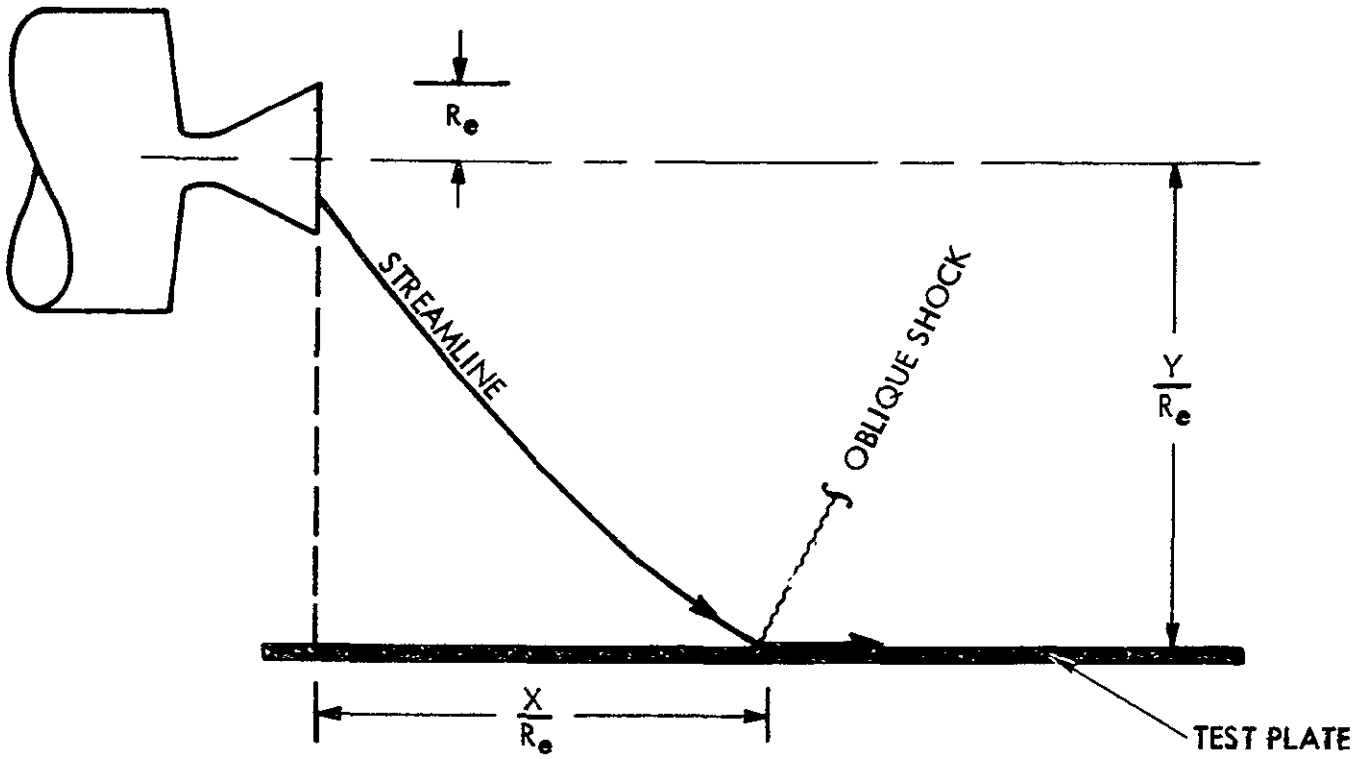

Figure 23. Pictorial Representation of the Normalized Coordinate System

layer on the angle of the Mach number line for the three thrusters is presented on Figure 30. Consequently, instead of a 76.96-degree initial boundary turning angle (noted on Figure 24), the plume boundary will expand greater than 162 degrees when boundary layer theory is applied. For example, note the position of the Mach 20 line on Figure 25. This line makes an initial angle of approximately 52 degrees with the nozzle centerline. However, when boundary layer theory is applied, this Mach line makes an angle of approximately 157 degrees with nozzle centerline (see Figure 30). The analytic method which gives the boundary layer expansion may be found in Reference 1. It should be noted that the method described in Reference 1 is a quick approximation analysis. More detailed and more accurate methods exist in the literature.

It should also be noted that the exhaust gas of a hydrazine thruster is calorically imperfect. As the gas expands, the specific heat ratio increases. The specific heat ratio values used in Figures 24 through 30 are based on engine chamber conditions. The use of these values will result in the largest

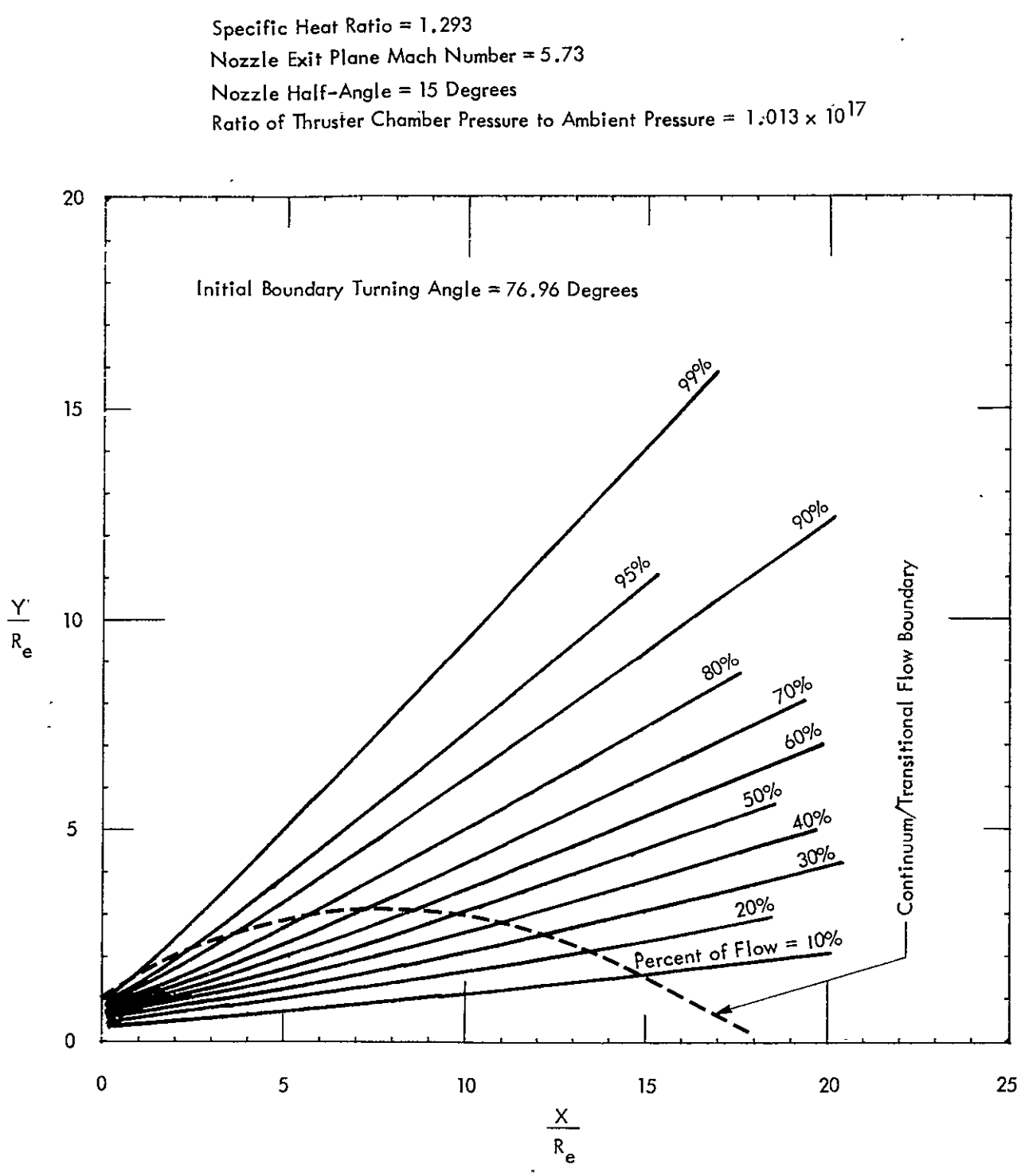

Figure 24. Hydrazine 0.2-lbf Thruster: Percent of Exhaust Plume Flow

Specific Heat Ratio = 1.293

Nozzle Exit Plane Mach Number = 5.73

Nozzle Half-Angle = 15 Degrees

Ratio of Thruster Chamber Pressure to Ambient Pressure = 1.013×10^{17}

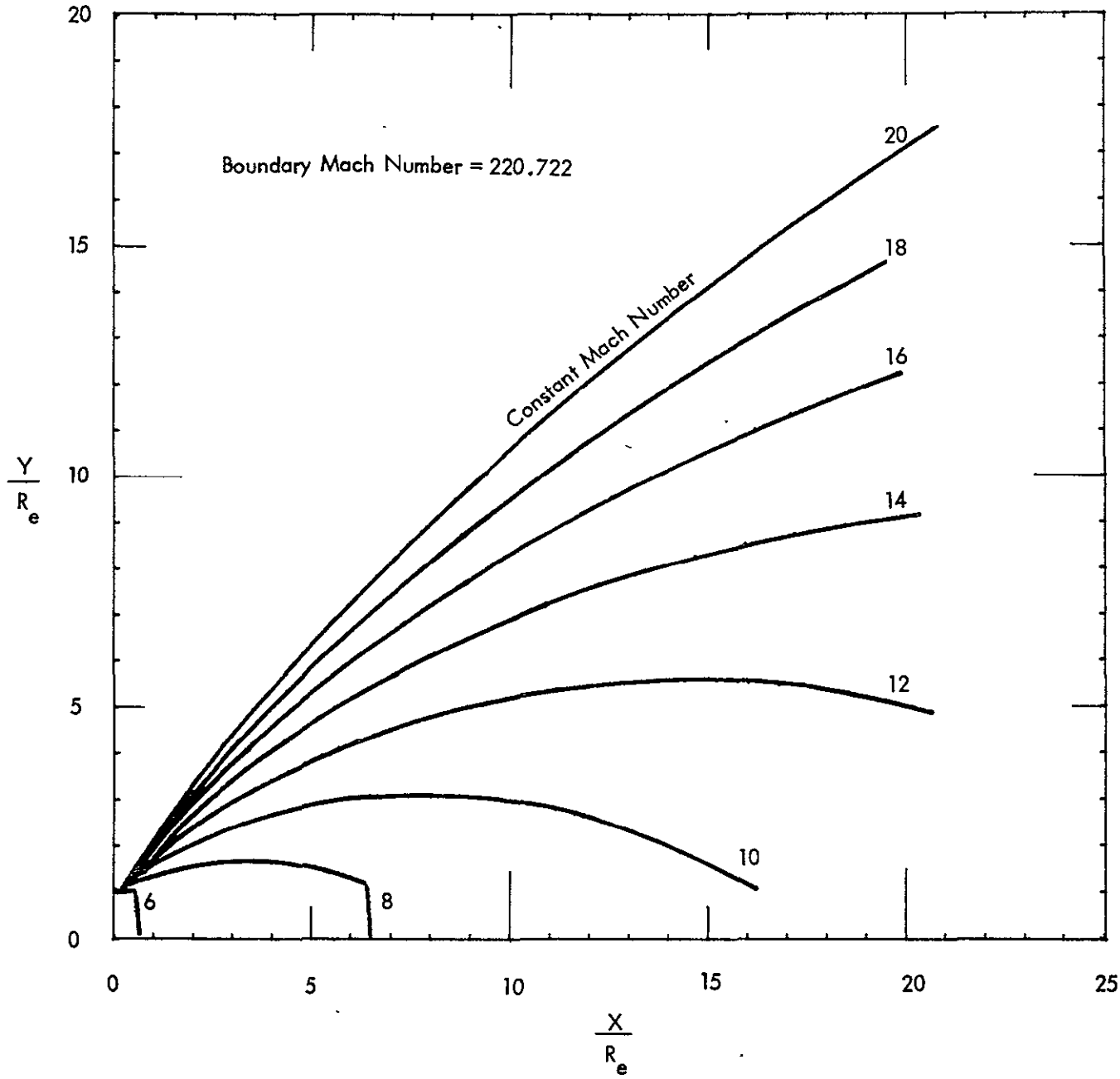

Figure 25. Hydrazine 0.2-lbf Thruster: ISO-Mach Graph

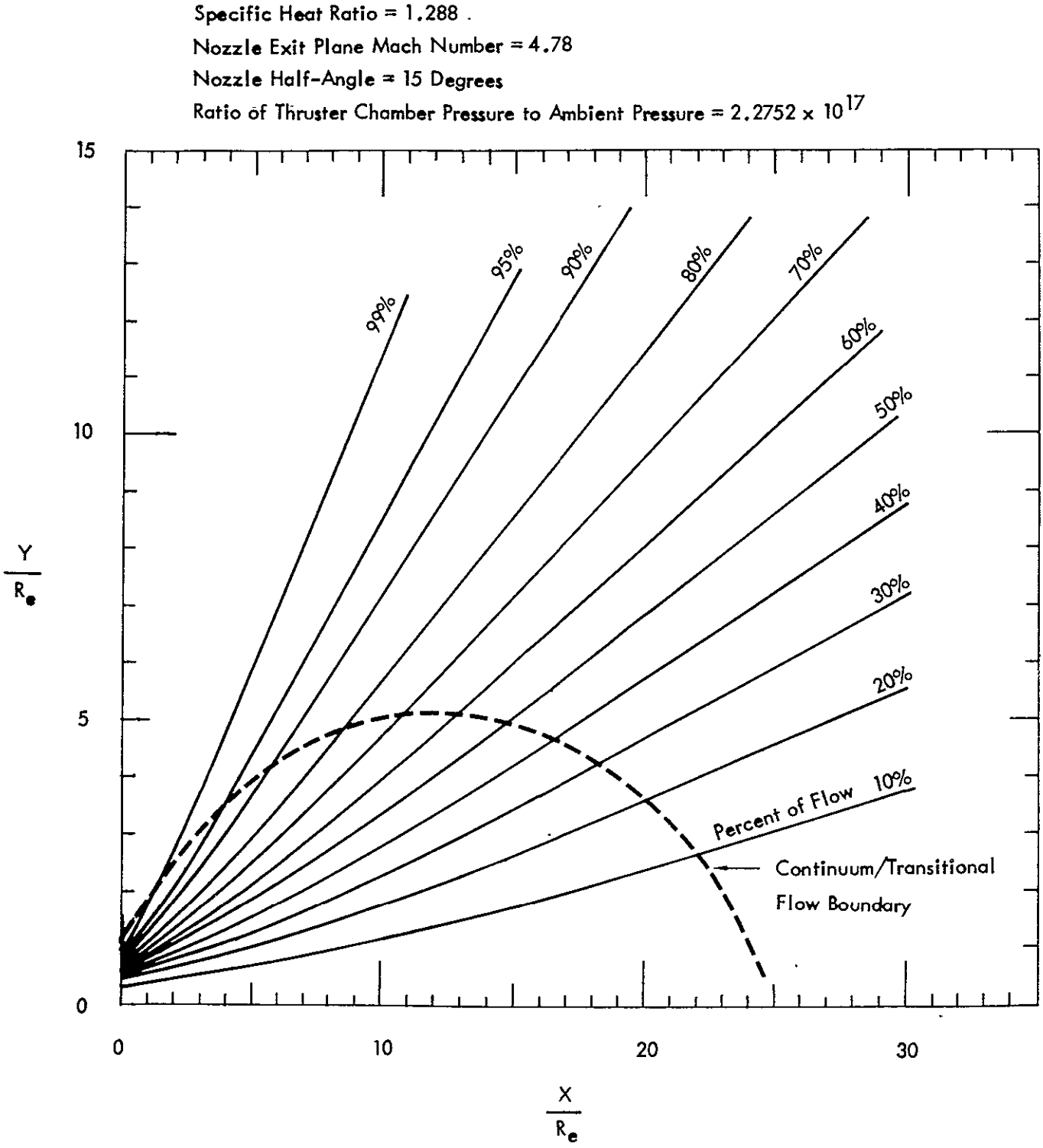

Figure 26. Hydrazine 5-lbf Thruster: Percent of Exhaust Plume Flow

Specific Heat Ratio = 1.288

Nozzle Exit Plane Mach Number = 4.78

Nozzle Half-Angle = 15 Degrees

Ratio of Thruster Chamber Pressure to Ambient Pressure = 2.2752×10^{17}

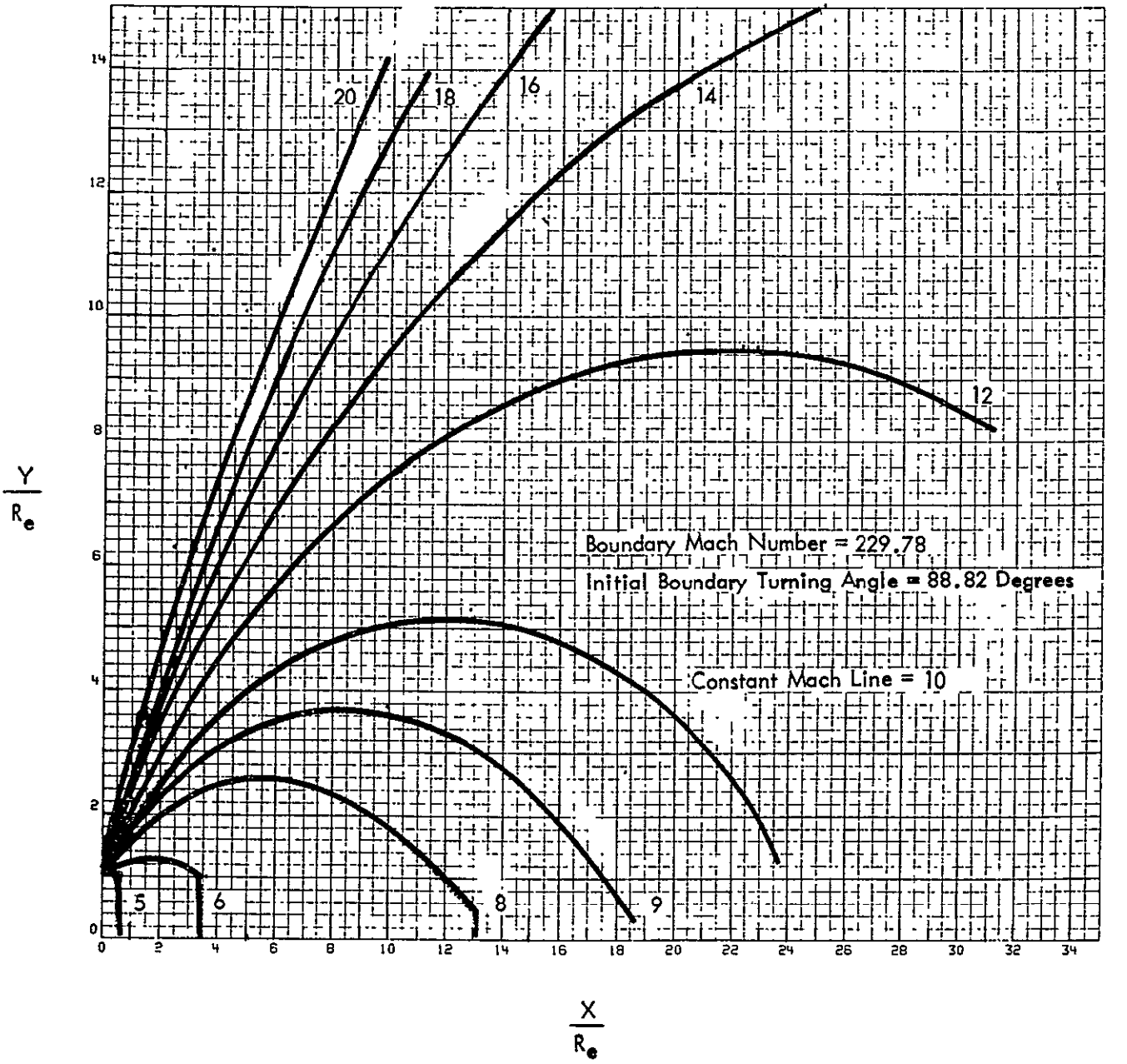

Figure 27. Hydrazine 5-lbf Thruster: ISO-Mach Graph

Specific Heat Ratio = 1.283
Nozzle Exit Plane Mach Number = 4.955
Nozzle Half-Angle = 15 Degrees
Ratio of Thruster Chamber Pressure to Ambient Pressure = 1×10^{18}

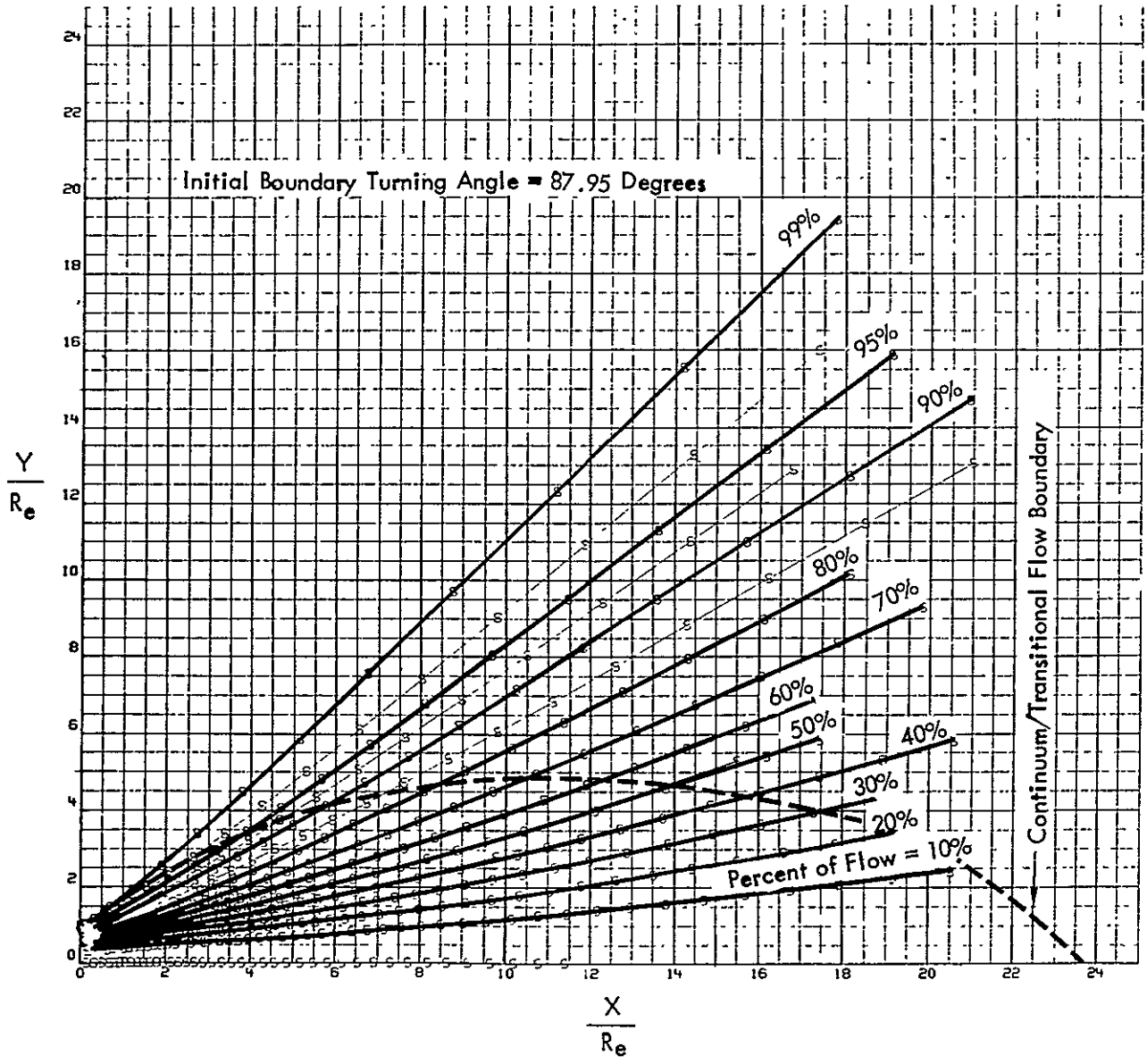

Figure 28. Hydrazine 100-lbf Thruster: Percent of Exhaust Plume Flow

Specific Heat Ratio = 1.283

Nozzle Exit Plane Mach Number = 4.955

Nozzle Half-Angle = 15 Degrees

Ratio of Thruster Chamber Pressure to Ambient Pressure = 1×10^{18}

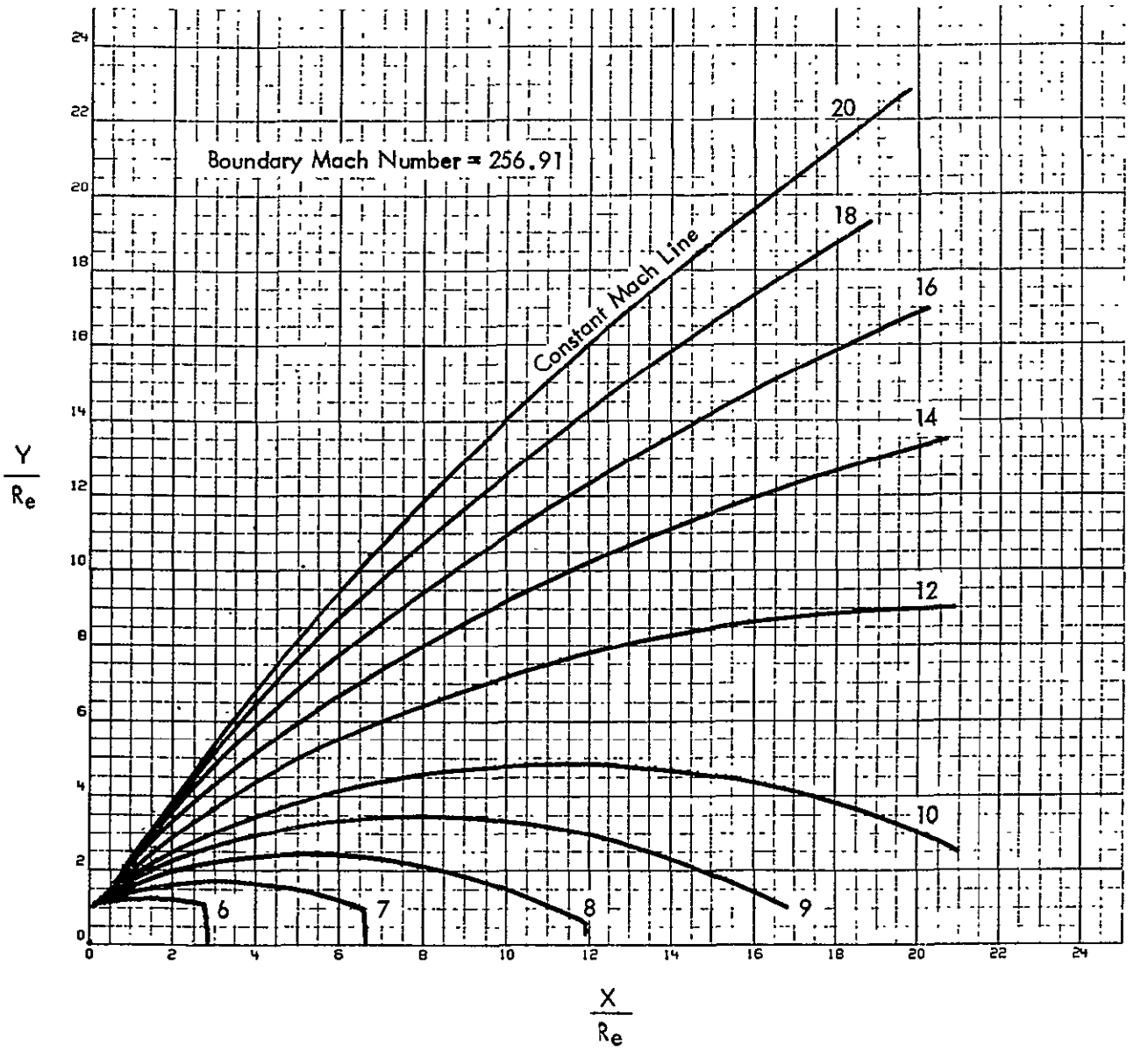

Figure 29. Hydrazine 100-lbf Thruster: ISO-Mach Graph

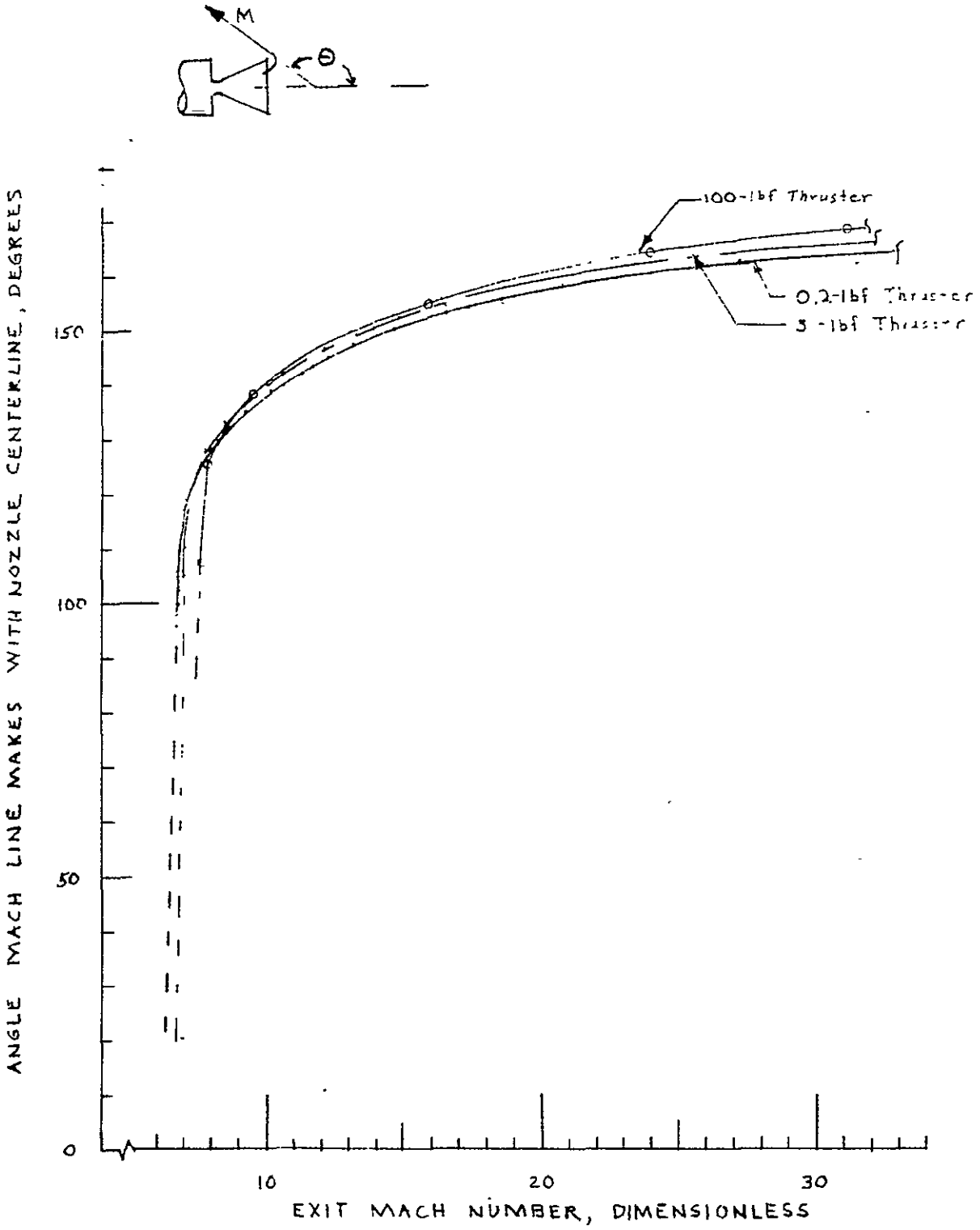

Figure 30. Mach Line Angle Using Boundary Layer Theory

plume and also the highest heat transfer rates and impingement pressures at any point within the plume. For conservative design purposes, the engine chamber specific heat ratio is the recommended value to be used.

Based on this analysis, the region of influence for all three thruster sizes is plus or minus 170 degrees as measured from the nozzle centerline. As stated, the larger the nozzle exit plane diameter, the smaller the amount of flow affected by the boundary layer.

The exhaust plume will impinge onto the Landsat-D solar array and TDRS antenna to some degree. There will be no buildup of contamination deposition on either item since the surfaces will be warmer than $-100^{o}F$ and the transmittance of the solar cells will not be significantly affected as a result of the exhaust plume impinging onto the surface. Heating rates of 1.6×10^{-4} to 4.3×10^{-5} BTU/FT^2-sec can be anticipated to exist on the solar array as a result of exhaust plume impingement when the array is nearest to the thrusters. Heating rates of 1.55×10^{-4} to 5.4×10^{-5} BTU/FT^2 -sec are predicted for the TDRSS antenna when it is pointing downward toward the thruster. For the solar array, a vector sum disturbance torque of 2.04×10^{-2} in-lbf (maximum) is predicted while the 0.2-lb thruster is firing and when the solar array is nearest the active thruster module. For the TDRSS antenna, a maximum disturbance torque of 2.06×10^{-2} in-lbf (maximum) is predicted when the antenna is pointing toward an active thruster. The thrusters could be canted to reduced the impingement but the analytical heat rates and disturbance torques are within the design limits of the system and the exposure times should be short.

6.2 BERTHING PROBE/ELECTRICAL CONNECTOR HEAT TRANSFER ANALYSIS

Because the berthing probe and the spacecraft side of the launch umbilical are well within the expected plume envelope for the SPS-I configuration, an investigation of the induced environment was made. Two methods were used to determine the impingement pressure and convective heat transfer rate onto the berthing probe tip and the top of the electrical connector (Figure 31). These two positions were selected because these points would have the maximum and minimum values of pressure and heat transfer rate for the electrical connector/probe assembly. The first method was developed primarily for nozzle back-flow problems but is considered applicable to this problem. The second method was developed for this type of flow problem (Reference 2). Table 10 presents the data required to use the two methods. The coordinate system is shown in Figure 32.

6.2.1 Nomenclature/Units

A_e/A^* = Nozzle area-to-throat ratio $(R_e/R^*)^2$, dimensionless

C^* = Characteristic velocity, ft/sec

F/F_{max} = Thrust coefficient, dimensionless

g_c = Gravitational constant, 32.17 lbm-ft/lbf-sec^2

I_1 = Plume integral, dimensionless

M = Mach number, dimensionless

η = Flow angle function, dimensionless

P = Impingement pressure, psia

P_c = Engine chamber pressure, psia

• BERTHING PROBE IMPINGEMENT

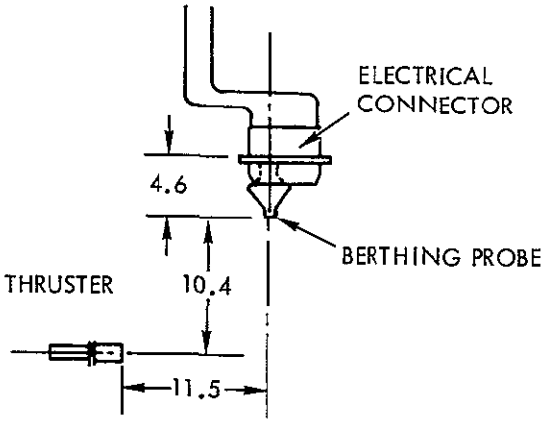

THRUSTER CHARACTERISTICS:

- EXPANSION RATIO (ϵ) - 100
- EXIT RADIUS (R_e) - 0.115-IN.
- NOZZLE HALF ANGLE (θ_η) - 15°

Figure 31. Spatial Relationship Between Hydrazine Thruster and Berthing Probe Assembly

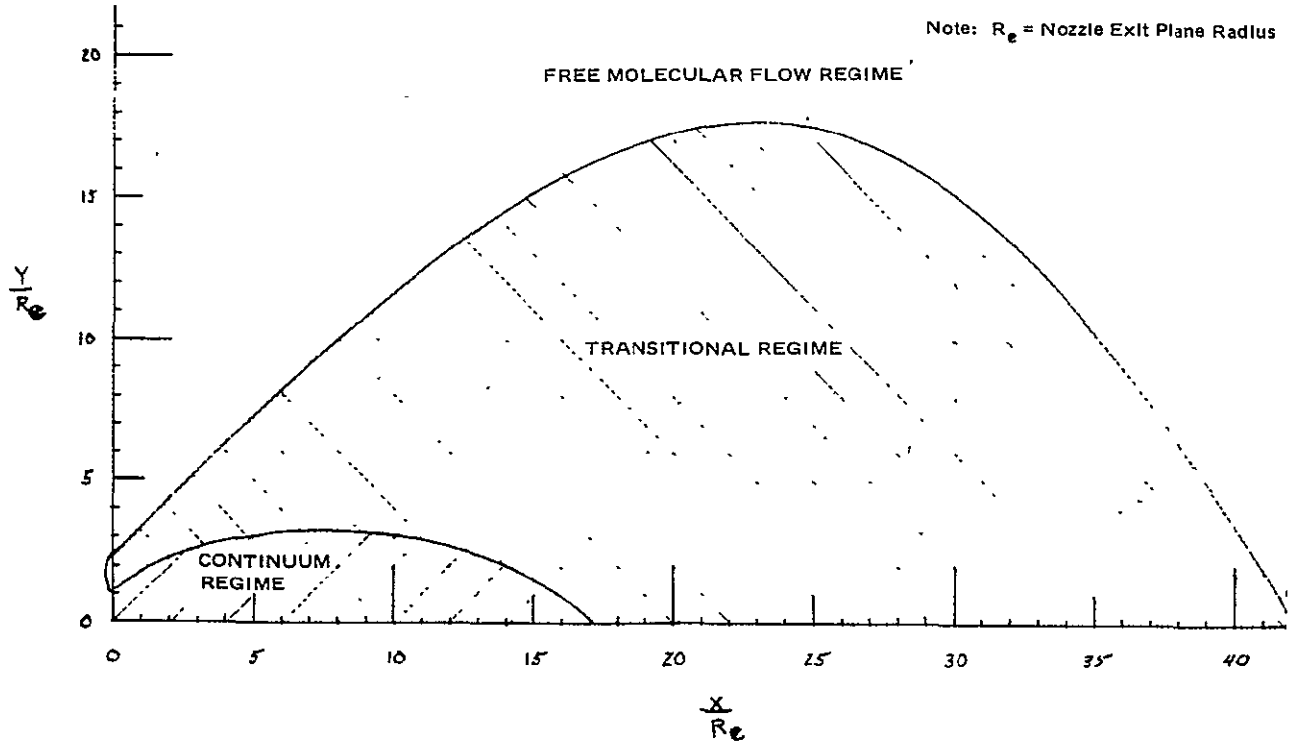

Figure 32. Graphical Representation of the Three Exhaust Plume Gas Flow Regimes for the 0.2-lbf Hydrazine Thruster in Space

Table 10. Pertinent Data

Item	Value
0.2-lbf N_2H_4 Engine Operating Conditions	
Assumed chamber pressure (Pc)	275 psia
Assumed ammonia dissociation	65.6%
• Gas chamber temperature (Tc)	2045° R
• Molecular weight	12.6 lb mass/lb-mole
• Specific heat ratio (γ)	1.293
Derived nozzle exit plane parameters assuming constant specific heat ratio and inviscid flow analysis	
• Mach number (Me)	5.73067
• Gas velocity (Ve)	7677.59167 ft/sec
• Static temperature (Te)	351.90973° R
• Static pressure (P_e)	0.11659 psia
• Static density (ρ_e)	3.89082×10^{-4} lbm/ft^3
Gas Constant (R)	122.61905 lbf-ft/lbm-°R
Coordinate System (see Figures 23 and 31)	
$\frac{X}{R_e}$ = 0 at nozzle exit plane	
$\frac{Y}{R_e}$ = 0 at nozzle centerline	
Berthing probe tip	
• $X/R_e = (37-25.5)/0.115 = 100$	
• $Y/R_e = (15-4.6)/0.115 = 90.4348$	
• Angle from nozzle centerline = $\tan^{-1}(y/x) = 42.1246°$	
• Angle from nozzle exit radius = $\tan^{-1}[(15-4.6-0.115)/(37-25.5)] = 41.8078°$	
Top of Electrical Connector	
• $X/R_e = (37-25.5-1.7)/0.115 = 85.2174$	
• $Y/R_e = (15-(-2.4)/0.115 = 151.304$	
• Angle from nozzle centerline = $\tan^{-1}(y/x) = 60.6109°$	
• Angle from nozzle exit radius = $\tan^{-1}[(17.4-.115)/(37-25.5-1.7)] = 60.4483°$	

P_e/P_* = Ratio of nozzle exit plume static pressure to nozzle throat static pressure, dimensionless

$\dot{Q}$ = Convective heat transfer rate, Btu/ft^2-sec

r_e/r_* = Ratio of nozzle exit plane radius to throat radius, dimensionless

T_c = Engine chamber temperature, °R

V = Gas velocity, ft/sec

V_{max} = Maximum velocity, ft/sec

V_*/V_{max} = Ratio of sonic velocity to maximum velocity, dimensionless

X/r_* = Ratio of X-distance to nozzle throat radius, dimensionless

y/r_e = Normalized distance perpendicular from nozzle centerline, dimensionless

α_K = Accommodation coefficient, dimensionless (assumed = 1)

β = Plume parameter, dimensionless

γ = Gas specific heat ratio, dimensionless (γ = 1.293)

θ = Angle of streamline with nozzle centerline, degrees

θ_η = Nozzle half-angle, degrees

ρ = Gas density of streamline, lbm/ft^3

λ = Plume parameter, dimensionless

Subscripts

B Denotes boundary layer conditions

P Denotes plume conditions

6.2.2 Analysis

Method 1 - Boundary Layer Method (Source: Reference 1)

- Maximum impingement pressure:

$$P_{impingement} = \frac{(\rho V^2)_B \left(\frac{M_P}{M_B}\right)^2 \left[\frac{1 + \left(\frac{\gamma-1}{2}\right) M_B^2}{1 + \left(\frac{\gamma-1}{2}\right) M_P^2}\right]^{\frac{\gamma}{\gamma-1}}}{g_c (144) \left(\frac{y}{R_e}\right)^2}$$

- Maximum convective heat transfer rate:

$$\dot{Q} = \frac{\left(\frac{1}{2}\rho V^3\right)_B \left(\frac{M_P}{M_B}\right)^3 \left[\frac{1+\left(\frac{\gamma-1}{2}\right) M_B^2}{1+\left(\frac{\gamma-1}{2}\right) M_P^2}\right]^{\frac{3\gamma-1}{2(\gamma-1)}}}{g_c\ (778)\ \left(\frac{y}{Re}\right)^2}$$

See Table 11 for parameters and results.

Method 2 - Free Molecular Flow Model (Reference 2).

$$B = 0.835 / (1 - F/F_{max})$$

$$\frac{F}{F_{max}} = \left(\frac{1+\cos\theta_n}{2}\right)\left(\frac{1+\gamma M_e^2}{\gamma}\right)\left(\frac{P_e}{P_*}\right)\left(\frac{A_e}{A_*}\right)\left(\frac{V_*}{V_{max}}\right)$$

$$\frac{P_e}{P_*} = \left[\frac{2+(\gamma-1)M_e^2}{\gamma+1}\right]^{-\frac{\gamma}{\gamma-1}}$$

$$\frac{V_*}{V_{max}} = \sqrt{\frac{\gamma-1}{\gamma+1}}$$

$$\gamma = B/4 \qquad I_1 = 0.905/B \qquad n = 1-\cos\theta$$

$$V_{max} = \sqrt{2\gamma g_c R T_c / (\gamma-1)}$$

$$C^* = \left[\frac{1}{\gamma}\left\{\frac{\gamma+1}{2}\right\}^{\frac{\gamma+1}{\gamma-1}} g_c R T_c\right]^{\frac{1}{2}}$$

Table 11. Method 1 Parameters

Item	Berthing Probe Tip	Top of Electrical Connector
Angle from nozzle exit radius	41.8078	60.4483
Normalized boundary layer streamline corresponding to plume streamline impinging surface $\frac{\delta}{R_e}$	2.8024×10^{-2}*	1.1415×10^{-2}*
M_B	4.8529*	3.7915*
M_P	8.1073*	8.6267*
V_B, ft/sec	5341.4788	3907.4092
ρ_B, lbm/ft^3	5.7543×10^{-4}	8.0332×10^{-4}
γ	1.293	1.293
y/Rc	90.4348	151.304
P, psia	2.5938×10^{-5}	1.5942×10^{-6}
$\dot{Q}$, Btu/ft^2-sec	1.3860×10^{-2}	6.7002×10^{-4}

*Previous analysis using this method

$$V_B = C_1 V_C \text{ and } \rho_B = C_2 \rho_e$$

Reynolds number at nozzle exit plane $= \left(\frac{\rho V R}{\mu}\right)_e$

$$= \frac{(3.8908 \times 10^{-4})(7677.59)(0.115/12)}{24 \times 10^{-6}}$$

$$R_e = 1192.811$$

$\delta_{max}/R_e = 2.326 (R_e)^{-0.29056}$ (from Reference 2) $= 0.296948$

C_1 and C_2 are functions of δ/δ_{max} (or $\delta/Re \div \delta_{max}/R_e$)

From Reference 1

For $\theta = 60.4483$, $\delta/\delta_{max} = 0.03844$ $C_1 = .5089$ $C_2 = 2.06465$

For $\theta = 41.8078$, $\delta/\delta_{max} = 0.09437$ $C_1 = .6957$ $C_2 = 1.47894$

$$\frac{x}{r_*}\sqrt{\frac{\rho V_{max} C^*}{P_c}} = \left[\frac{e^{-n(\lambda^2 n + B)/2}}{\sqrt{2 I_1}}\right]^{(1-n)}$$

$$P = \frac{\rho V_{max}^2 \sin^2\theta}{g_c\ 144} = \left[\frac{x}{r_*}\sqrt{\frac{\rho V_{max} C^*}{P_c}}\right]^2 \left(\frac{P_c}{C^*}\right) \frac{\sin^2\theta\ V_{max}}{\left(\frac{x}{Re}\right)^2 \left(\frac{R_c}{r_*}\right)^2 g_c\ 144}$$

$$\dot{Q} = \frac{\alpha_K \left(\frac{1}{2}\rho V_{max}^3\right)\cos\theta}{g_c\ 778} = \left(\frac{\alpha_K P}{2}\right)\left[\frac{144}{778}\right] V_{max}\ \frac{\cos\theta}{\sin^2\theta}$$

See Table 12 for parameters and results

Table 12. Method 2 Parameters

Item	Berthing Probe Tip	Top of Electrical Connector
Angle from nozzle centerline, deg.	42.1246	60.6109
Specific heat ratio, γ	1.293	1.293
Ae/A* or $(R_e/R^*)^2$	100	100
V*/Vmax	0.35746	0.35746
Pe/Px	7.7509×10^{-4}	7.7509×10^{-4}
θn, deg.	15	15
F/Fmax	0.91546	0.91546
B	9.8775	9.8775
λ	2.4694	2.4694
I_1	9.16228×10^{-2}	9.16228×10^{-2}
θ, deg.	42.1246	60.6109
n	0.25831	0.50926
$(x/R^*)\sqrt{\rho V_{max} C^*/P_c}$	0.39474	0.04204
Vmax, ft/sec	8437.846	8437.846
C*, ft/sec	4264.624	4264.624
Pc, psfa	39600	39600
P, impingement pressure, psia	1.18568×10^{-6}	3.1245×10^{-8}
$\dot{Q}$, heat rate, Btu/ft-sec	1.52636×10^{-3}	1.57715×10^{-5}

Note:

$\frac{x}{R_e}$ = 100 for berthing probe tip

$\frac{x}{R_e}$ = 85.2174 for electrical connector top

6.2.3 Plume Impingement Issues

No contamination problems resulting from plume impingement on the umbilical connector are anticipated based on the following rationale.

The possible sources of contamination are the small amounts of aniline and water present in the propellant and any unreacted hydrazine. When exposed to the catalyst bed, aniline probably becomes a hydrocarbon and water may remain water or become an ammonium hydrate. These elements are the potential contamination sources because they condense at much higher temperatures than the main constituents of the exhaust plume, i.e. ammonia, hydrogen, and nitrogen.

Contamination measurements have been made using a 0.1-lbf hydrazine thruster and quartz micro-balances located 44 inches from the nozzle exit plane (see Reference 3). Although no test specimen was located beyond a 30 degree angle from the nozzle centerline, the data obtained from the reference can be used as an upper limit. Recall that the berthing probe tip is at an angle of 42 degrees with the nozzle certerline and the top of the electrical connector is at an angle of 60 degrees with the nozzle centerline.

Using the data from Reference 3, the following observations can be made:

1. No mass deposition occurs if the surface temperature is warmer than $410^{\circ}R$ (applicable to all angles).
2. Deposition rate increases with a decrease in temperature.
3. Thruster usage (i.e., aging) decreases deposition rate.
4. Specific data for test specimen located at 30 degrees (steady-state):
   (a) Deposition rate = 3×10^{-12} gm/cm^2-sec at $360^{\circ}R$
   (b) Deposition rate = 1×10^{-9} gm/cm^2-sec at $259.2^{\circ}R$
   (c) Deposition rate = 3×10^{-8} gm/cm^2/sec at $190.8^{\circ}R$
5. Pulsing decreases the deposition rate by an order of magnitude.
6. A water content increase from 0.7% to 1.8% increases the deposition rate by an order of magnitude.

The umbilical connector will ordinarily be warmer than $-50^{\circ}F$ for the Landsat mission;consequently, no deposition will occur. However, there could be other missions when the umbilical connector temperature is as cold as $-100^{\circ}F$ (worst case). If the thruster operates during this time period, a deposition rate no greater than 3×10^{-12} $gm.cm^2$-sec can be anticipated. Assuming the surface area is 155 cm^2, the resulting deposition rate is 4.65×10^{-10} gm/sec. The engine could operate more than 100 hours continuously and the resulting deposition would still be insignificant. This, of course, is orders of magnitude longer than anticipated.

6.3 GRAPHICAL METHODS

Several graphs have been developed from the analytical methods which allow the evaluation of the impingement pressure and convective heat transfer effects from the exhaust plume of a 0.2-lbf hydrazine thruster onto surfaces within the free molecular flow regime without requiring many calculations. It should be noted that the results are approximations.

6.3.1 Limitations and Assumptions

1. Figures 33 and 34 apply only to the free molecular flow regime described in Figure 32.
2. The flow angle, θ, has its apex at the intersection of the nozzle centerline and the nozzle exit plane (i.e., $X/R_e = Y/R_e = 0$) with one side of the angle being the nozzle centerline and the remaining side being a ray from the apex to the object in question.
3. The distance, y, is the length of the line between the surface in question and the nozzle centerline. This line is perpendicular to the nozzle centerline.
4. The 0.2-lbf N_2H_4 thruster was assumed to have the following characteristics and operating conditions:
   - Chamber pressure - 275 psia
   - Chamber temperature - 2045°R
   - Expansion ratio - 100
   - Nozzle exit plane radius = 0.115 inch
   - Nozzle half-angle - 15°
5. The exhaust gas was assumed to have a constant specific heat ratio equal to 1.293 and gas constant = 122.619 lbf-ft/lbm-°R.
6. Ratio of chamber pressure to ambient pressure is 1.013×10^{17}. Consequently, Figures 33 and 34 apply to space conditions only.

References:

1. French, E.P., Dr.: Plume Heating by GPS Orbital Insertion Motor. AT/EF/76-003, Rockwell International/Space Division Internal Letter dated 22 January 1976
2. French, E.P., Dr.: Rocket Plume Effects in Space. SD74-SA-0137, Rockwell International/Space Division, Downey, California, October 1974.

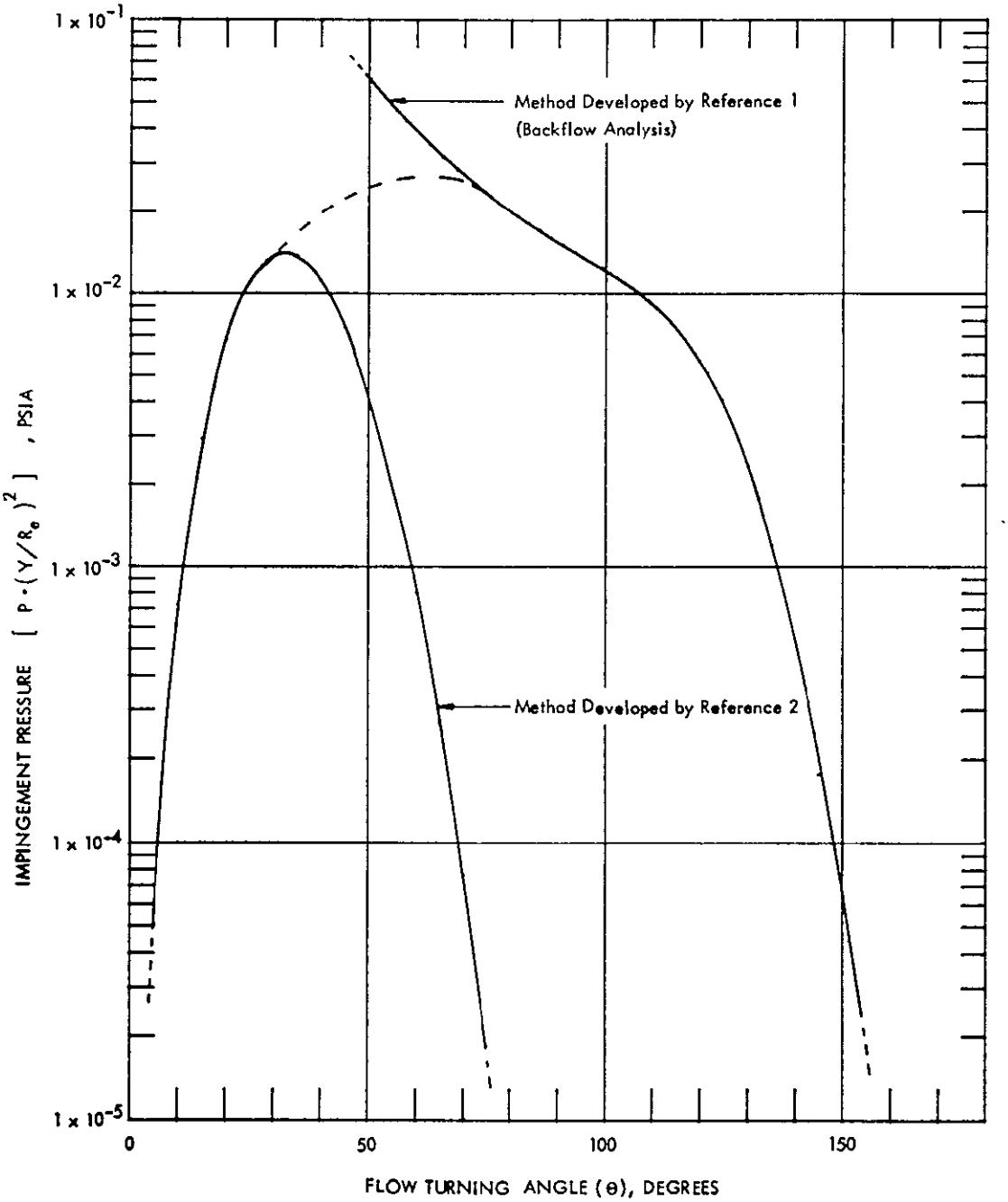

Figure 33. Hydrazine 0.2-lbf Thruster Exhaust Plume Free Molecular Flow Impingement Pressure as a Function of Flow Angle

References:

1. French, E.P.,Dr.: Plume Heating by GPS Orbital Insertion Motor. AT/EF/76-003, Rockwell International/Space Division Internal Letter dated 22 January 1976.
2. French, E.P., Dr.: Rocket Plume Effects in Space. SD74-SA-0137, Rockwell International/Space Division, Downey, California, October 1974.

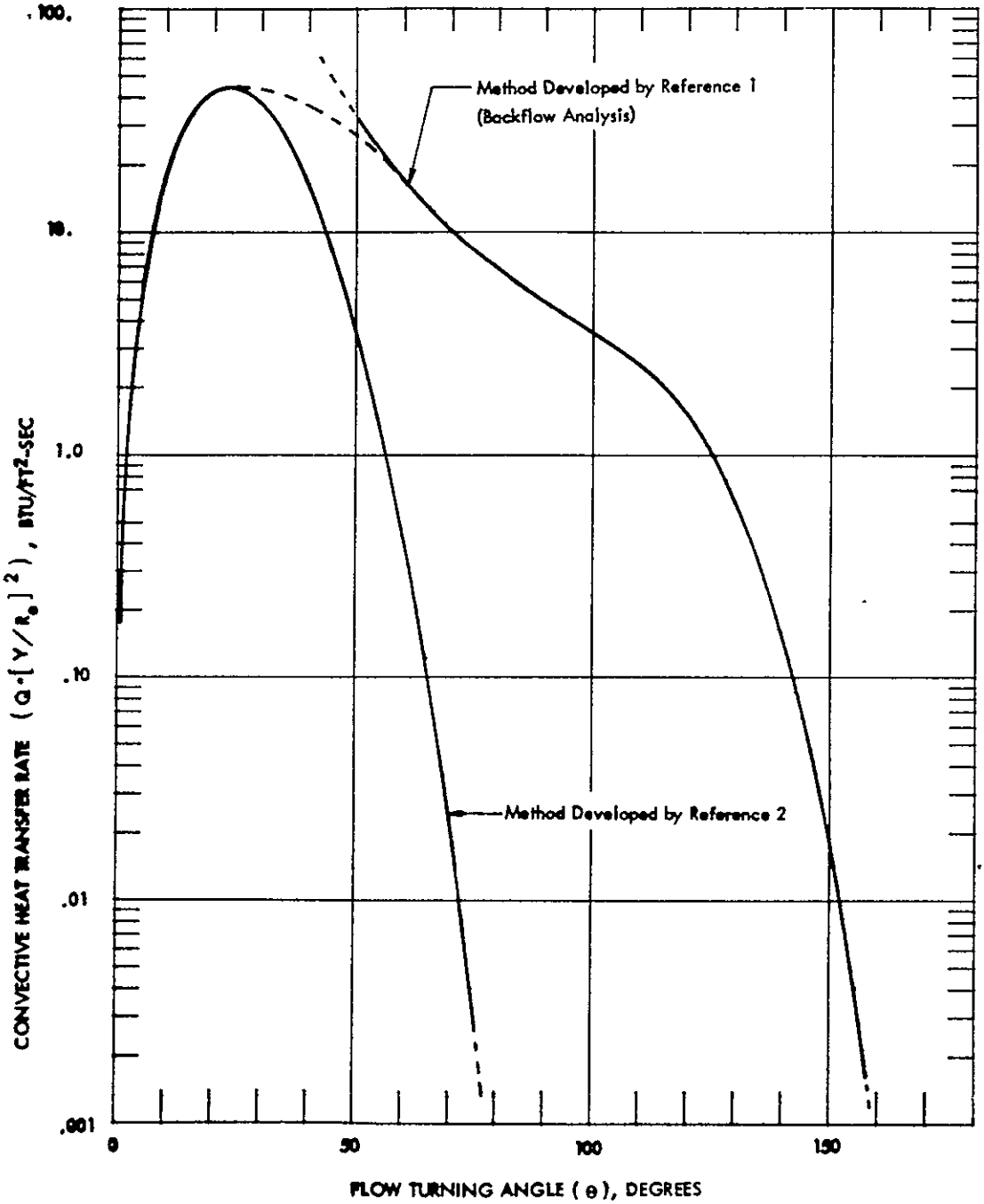

Figure 34. Hydrazine 0.2-lbf Thruster Exhaust Plume Free Molecular Flow Convective Heat Transfer Rate as a Function of Flow Angle

6.3.2 Sample Calculation for Berthing Probe Tip

$$\frac{X}{R_e} = 100\,\frac{Y}{R_e} = 90.43 \qquad \text{(from Table 10)}$$

From Figure 32, the berthing probe tip is in the free molecular flow regime.

$$\theta = 41.80° \qquad \text{(from Table 10)}$$

From Figure 33, $P\left(\frac{Y}{R_e}\right)^2 = .021$ psia

$$P = \frac{.021}{\left(\frac{Y}{R_e}\right)^2} = \frac{.021}{(90.43)^2} = 2.568 \times 10^{-6} \text{ psia}$$

From Figure 34, $\dot{Q}\left(\frac{Y}{R_e}\right)^2 = 36$ Btu/ft^2-sec

$$\dot{Q} = \frac{36}{(90.43)^2} = 4.402 \times 10^{-3} \text{ Btu/ft}^2\text{-sec}$$

Comparing with the previous methods results in the following:

	Method 1	Method 2	Graphical
Impingement pressure, psia	2.6×10^{-5}	1.2×10^{-6}	2.6×10^{-6}
Convective heat transfer rate, Btu/ft^2-sec	1.4×10^{-2}	1.5×10^{-3}	4.4×10^{-3}

The graphical method answer is between the other two answers, as might be anticipated by examining either Figure 33 or 34. The point selected lies on the transitional line; it is not on either loci of points generated by Method 1 or Method 2.

For conservative design purposes, a factor of 2 over the maximum value probably should be used. Following this philosophy, the berthing probe assembly should be designed to withstand a convective heat transfer rate from the exhaust plume of 0.028 Btu/ft^2-sec. Should this heat rate cause design problems, a more detailed heat transfer analysis should be performed.

7.0 REFERENCES

6-1. French, E. P.: Plume Heating by GPS Orbital Insertion Motor. AT/EF/76-003, Rockwell International/Space Division Internal Letter, dated 22 January 1976.

6-2. French, E. P.: Rocket Plume Effects in Space. SD 74-SA-0137, Rockwell International/Space Division, Downey, California, October 1974.

6.3 Passamaneck, R.S. and Chirivella, J.E.: Contamination Measurements For a 0.1 LBF Monopropellant Thruster. CPIA Publication 277, JANNAF 9th Plume Technology Meeting, Chemical Propulsion Information Agency, John Hopkins University, Applied Physics Laboratory, Silver Spring, Md., April 1976 (pp. 353-376).